Department of Physics and Astronomy

University of Heidelberg

Master thesis

in Physics

submitted by

Juliana Stachurska

born in Berlin

2014

Sterile Neutrinos

in Extra Dimensions

as Warm Dark Matter Candidates

This Master thesis has been carried out by Juliana Stachurska

at the

Max-Planck-Institute for Nuclear Physics

under the supervision of

Dr. Werner Rodejohann

Abstract

Many years after it has been established that most of the matter density in the universe is made up of some form of dark matter, its nature remains a mystery. The consensus is that dark matter is non-baryonic, and for a long time it was widely believed that it has to be dynamically cold to allow for structure formation at early times in the universe. However, it now seems like warm dark matter may alleviate tensions between observations and simulations based on theoretical predictions from cold dark matter driven structure formation, especially on smaller, sub-galactic scales. Sterile neutrinos arise in a variety of extensions of the Standard Model of particle physics, and can be used to generate a neutrino mass term or account for short baseline oscillation anomalies depending on their mass in the given scenario. They are also very good candidates for warm dark matter. Here, we present one such Standard Model extension, featuring a large compactified extra dimension, and study how the tower of sterile neutrino Kaluza-Klein modes arising in this setting affects the sterile neutrino properties. In particular, we focus on its influence on the sterile neutrino abundance, if it is to match the dark matter abundance, and possible signatures both in astrophysical observations and in nuclear β-decay. We find that the extra dimensional setting only insignificantly changes both production and signatures of sterile neutrinos, and conclude that if existing, the additional Kaluza-Klein modes will most likely remain hidden for many years to come.

Zusammenfassung

Seit vielen Jahren ist bekannt, dass die meiste Materiedichte im Universum in der Form von Dunkler Materie vorliegt. Der Konsens ist, dass Dunkle Materie nicht-baryonisch ist. Lange Zeit über war die gängige Überzeugung, dass Dunkle Materie dynamisch kalt sein muss, um Strukturbildung im frühen Universum zu ermöglichen. Auf subgalaktischen Skalen jedoch gibt es Unterschiede zwischen den Simulationen, basierend auf theoretischen Vorhersagen der Strukturbildung für Kalte Dunkle Materie, und Beobachtungen, welche durch Warme Dunkle Materie behoben werden könnten. Sterile Neutrinos sind ein Teil mehrerer Erweiterungen des Standardmodells der Teilchenphysik, und können je nach ihrer Masse im jeweiligen Szenario die Massenerzeugung bei Neutrinos oder auch Anomalien vieler verschiedener Neutrinooszillationsexperimente erklären. Sie sind auch sehr gute Kandidaten für Warme Dunkle Materie. Hier präsentieren wir eine dieser Standardmodellerweiterungen, und zwar eine mit einer zusätzlichen, großen, kompaktifizierten Dimension. Wir untersuchen die Auswirkungen des sich aus der Zusatzdimension ergebenden Turms von Kaluza-Klein Moden der sterilen Neutrinos. Wir konzentrieren uns auf die Auswirkungen auf die Energiedichte der sterilen Neutrinos, wenn diese der Energiedichte der Dunklen Materie entsprechen soll, sowie auf mögliche Signaturen bei astrophysikalischen Beobachtungen wie auch beim nuklearen β-Zerfall. Wir stellen fest, dass das extradimensionale Szenario die Produktion und die Signaturen von sterilen Neutrinos nur insignifikant beeinflusst. Wir schlussfolgern, dass die zusätzlichen Kaluza-Klein Moden, wenn sie existieren, wahrscheinlich viele weitere Jahre untentdeckt bleiben werden.

Contents

List of abbreviations

ADD	—	Arkani-Hamed–Dimopoulos–Dvali
BBNS	—	Big Bang Nucleosynthesis
CDM	—	Cold Dark Matter
DM	—	Dark Matter
DW	—	Dodelson–Widrow
ED	—	extra dimension
FIMP	—	Feebly Interacting Massive Particle
GUT	—	Grand Unified Theory
HDM	—	Hot Dark Matter
KK	—	Kaluza–Klein
ΛCDM	—	Standard Model of Cosmology with CDM and cosmological constant
LED	—	large extra dimension
LH	—	left-handed
LSS	—	Large Scale Structure
MSW	—	Mikheev–Smirnov–Wolfenstein
PMNS	—	Pontecorvo–Maki–Nakagawa–Sakata
RH	—	right-handed
SF	—	Shi–Fuller
SM	—	Standard Model
UED	—	universal extra dimension
vev	—	vacuum expectation value
WDM	—	Warm Dark Matter
WIMP	—	Weakly Interacting Massive Particle

Chapter 1

Introduction

One of the greatest mysteries of particle physics and cosmology is the still unknown nature of Dark Matter (DM). Even though it was established long time ago that the majority of matter in the universe is dark and non-baryonic, its nature remains a mystery. There have been several theories proposed to this day, that offer a more or less successful description of the DM. A successful DM model needs to explain the rotational curves of galaxies, the Large Scale Structure (LSS) formation, the interaction of galaxies in clusters, and the remarkably small number of observed satellite galaxies. Further, it has to be compatible with the observed abundance of elements, as described by the Big Bang Nucleosynthesis (BBNS). A hot, relativistic particle is ruled out as the prime constituent of the DM, as it would smear out structures and is incompatible with structure formation. Therefore, it is usually assumed that we live in a Cold Dark Matter (CDM) universe with Dark Energy, as described by the Standard Model of Cosmology, the ΛCDM model. A promising candidate for CDM is the Weakly Interacting Massive Particle, in short WIMP, which is a non-baryonic elementary particle, able to interact weakly (or, on the scale of the weak force) with Standard Model particles, and quite massive. A lot of effort has been dedicated to find WIMPs in recent years, and much of the parameter space of a WIMP has been excluded by now (see e.g. [1]). CDM can predict the LSS of the universe very well. On large scales, the predicitons of a ΛCDM universe are in excellent agreement with observations. However, the model has its shortcomings: CDM predicts too much power on smaller scales – it clumps too much, leading to many smaller than galactic structures like satellite galaxies. Also, it predicts cusped profiles for galactic gravitational potentials. Both predictions are inconsistent with observations: the discrepancy in the observed vs. predicted number of satellites is often referred to as the "missing satellite problem" while the discrepancy in the galactic gravitational pro-

files is often called the "cusp-vs.-core problem. A further shortcoming is the fact that so far, WIMPs have not been confirmed to exist by experiment.
One way to solve these problems is to assume a DM particle that is "warmer" than CDM and therefore named Warm Dark Matter (WDM). "Warmer" means, that the particle becomes non-relativistic at later times and has a larger free-streaming length as compared to CDM. Therefore, the formation of smaller objects such as satellite galaxies is suppressed. The small-scale suppression also would predict much smoother, cored gravitational profiles of galaxy halos, thereby being consistent with observations on small scales. For WDM, the particles become non-relativistic at later epochs, thus structure formation is delayed as compared to CDM. Observations of the structure formation history give limits on the free-streaming length, and thus the mass of thermal WDM. It is therefore required that on larger scales, WDM and CDM behaves alike (i.e. the WDM is not too warm), such that WDM can solve the problems we have so far on small scales, while recreating the large scale behaviour of CDM.

The Standard Model (SM) of Particle Physics is tremendously successful in explaining what elementary particles the matter we are surronded by is composed of, how these particles interact with each other and how they obtained their mass. And ever since the Higgs boson has been experimentally confirmed in 2012, the Standard Model can be regarded as complete. However, despite this model's great success, some open questions remain.
The Standard Model particle content only has three DM candidates, the three neutrinos. They interact weakly and could account for a "hot" component of the DM. But a Hot Dark Matter universe is ruled out. So, the SM has no answer to the question of the nature of DM. Also, in the SM, neutrinos are massless and only left-handed (LH). Right-handed (RH) neutrinos do not exist in the model. But today we know that neutrinos oscillate. The oscillation parameters are closely linked to mass differences between the neutrino mass eigenstates, and therefore neutrinos must have mass. However, their mass is so tiny, that only upper limits from direct mass measurements exist today, as well as a theoretical lower limits set by the mass differences measured in neutrino oscillation experiments [2, 3]
By introducing right-handed neutrinos to the SM, a mass term for neutrinos becomes possible. Right-handed neutrinos are sterile under the weak interaction, which makes them completely sterile under Standard Model interactions. However, via a small mixing with the active neutrinos they can couple to Standard Model particles.
Light sterile neutrinos can offer an explanation for the short baseline oscillation anoma-

lies, heavy massive neutrinos can account for the generation of neutrino mass, while sterile neutrinos of intermediate mass could make up a significant part of the Dark Matter in our universe. We will investigate the latter possibility of keV sterile neutrinos making up the Warm Dark Matter, and their observability, as WDM does not have the missing satellite problem and the cuspy halo problem that CDM models face.
There has recently been a claim of an unidentified 3.55 keV line in a stacked sample of galaxy clusters made by two independent groups [4, 5]. This line would be consistent with the radiative decay of a sterile neutrino with a mass of 7.1 keV to an active neutrino and a photon. While this claim has yet to be confirmed (or, possibly refuted) by new measurements, this mass range is an excellent starting point and further motivation for this thesis. We will investigate how sterile neutrino WDM could have been generated in the Early Universe, and what experimental signatures it has. Some extensions of the SM call for extra spatial dimensions. To leave the laws of gravity unchanged on larger scales, the extra dimensions (ED) have to be compactified. In the model proposed by Arkani-Hamed, Dimopoulos and Dvali (ADD) [6], SM particles are confined to the four-dimensional brane. Since sterile neutrinos have no interactions with the SM, they are free to probe the EDs of the bulk. In a setting with compactified extra dimensions, the mass of the sterile neutrinos depends on the radius of the ED. Thus, a wide range of masses is equally natural.

This thesis is organized as follows: In chapter 2, we will give a brief introduction into neutrino mixing and explain how it changes with the presence of extra dimensions. In chapter 3, the mechanisms of sterile neutrino DM generation are reviewed and applied to our case in chapter 4. The signatures of sterile neutrinos are presented in chapters 5 and 6 and we conclude in chapter 7. We will work in natural units, where $\hbar = c = k_B = 1$.

Chapter 2

Neutrinos in extra dimensions

In the SM, there are no RH neutrinos, making neutrinos the only fermions with only one chiral version. Introducing RH neutrinos as singlets into the framework of the SM makes the fermionic content symmetric. It also allows for a mass term for neutrinos, albeit the question of why neutrinos have a mass so much smaller than the other fermions still requires attention. Sterile neutrinos are used to account for various effects. As their mass is unrestricted by any known mechanism, they can have any mass that seems suitable for a model. Therefore, there are many different models with sterile neutrinos currently on the market. Light sterile neutrinos with masses around ~ 1 eV can explain the anomalies of various neutrino oscillation experiments – the LSND [7], MiniBooNE [8], reactor antineutrino [9] and gallium [10] anomalies. They can be globally fit if the existence of two sterile neutrinos with mass of the order of 1 eV is assumed [11]. However, they are not compatible with the Planck-mission results, according to which there are 3.30 ± 0.27 [12] effective neutrino-like relativistic degrees of freedom. Heavy sterile neutrinos can explain the tiny active neutrino masses generated by the seesaw-mechanism and have masses of the order of $\sim 10^{15}$ GeV [13]. And finally keV mass sterile neutrinos serve as a promising candidate for WDM. We will focus on the latter, and pair them with one large extra dimension (LED). This will not only introduce a mass scale, but also lead to the appearance of an infinite tower of sterile neutrinos, which may or may not have observable consequences.

2.1 Right-handed neutrinos as an extension of the Standard Model

In the SM, neutrinos are the only fermions that come only in the left-handed (LH) version which automatically excludes them from the possibility of having a mass generated in the same way as the other fermions. For the other fermions, the mass is generated via their Yukawa interaction with the Higgs field [14]:

$$\mathcal{L}_Y = -\overline{u}_{L,i} y_{u,i} \tilde{\Phi} u_{R,i} - \overline{d}_{L,i} y_{d,i} \Phi d_{R,i} - \bar{\ell}_{L,i} y_{l,i} \Phi \ell_{R,i} + h.c., \tag{2.1}$$

where $\tilde{\Phi} = i\sigma_2 \Phi^*$. Φ is the Higgs doublet, the u_i and d_i are the up- and downtype quarks respectively, and ℓ_i the charged leptons, i is the generation index and y are the Yukawa couplings. After spontaneous symmetry breaking, the Higgs field aquires a vacuum expectation value (vev), and the mass terms then read:

$$\mathcal{L}_m = -\overline{u}_{L,i} y_{u,i} \frac{v}{\sqrt{2}} u_{R,i} - \overline{d}_{L,i} y_{d,i} \frac{v}{\sqrt{2}} d_{R,i} - \bar{\ell}_{L,i} y_{l,i} \frac{v}{\sqrt{2}} \ell_{R,i} + h.c. \tag{2.2}$$

with mass terms $m_f = y_f \frac{v}{\sqrt{2}}$ and f is any of the massive fermions. Obviously, the above equation needs left- and righthanded fermions of the same type and therefore cannot be written down analogously for neutrinos. Neutrinos being LH in the SM only makes sense because they are also assumed to be massless. However, from the observation of neutrino oscillations we now know that neutrinos do have a tiny mass, thus the Standard Model is known to be incomplete and has to be extended. As neutrinos have a mass that is orders of magnitude smaller than the masses of the other fermions, it also seems unlikely that their mass is generated by the standard Higgs-mechanism. One way to generate neutrino mass is to introduce a Higgs triplet field Δ, which couples to LH neutrinos. After obtaining a vev (in analogy to the Higgs doublet) the Higgs triplet gives neutrinos mass via the Type-II Seesaw mechanism. The vev of the Higgs triplet is then assumed to be much smaller than the vev of the Higgs doublet, accounting for the tiny resulting neutrino masses. Instead of extending the bosonic content of the SM, one can take a different approach and extend the fermionic content by adding RH neutrinos. In any case an extension is necessary.

In the Type-I Seesaw mechanism, which does need RH neutrinos, the resulting neutrino mass term is

$$\mathcal{L}_m \supset -\overline{\nu_{L,i}} y_{D,i} \tilde{\Phi} \nu_{R,i} - \frac{1}{2} \overline{\nu^c_{R,i}} m_{R,i} \nu_{R,i} + h.c, \tag{2.3}$$

where we now have a Dirac mass $m_D = y_D \frac{v}{\sqrt{2}}$ and a Majorana mass m_R. In this case the mass matrix for the neutrino mass is,

$$\mathcal{M} = \begin{pmatrix} 0 & m_D \\ m_D & m_R \end{pmatrix}. \tag{2.4}$$

Diagonalising this mass matrix using the rotation matrix

$$\mathcal{O} = \begin{pmatrix} \cos\theta & -\sin\theta \\ \sin\theta & \cos\theta \end{pmatrix} \tag{2.5}$$

with $\tan\theta = 2m_D/m_R$ one finds $\mathcal{O}\mathcal{M}\mathcal{O}^T = diag(\lambda_-, \lambda_+)$ with the eigenvalues

$$\lambda_\pm = \frac{1}{2} m_R \pm \sqrt{m_R^2 + 4m_D^2}. \tag{2.6}$$

Under the assumption that $m_D \ll m_R$ the light active neutrino mass is then $m_\nu = |\lambda_-| \approx \frac{m_D^2}{m_R}$ and the heavy seesaw mass is $M = \lambda_+ = m_R + \frac{m_D^2}{m_R} \approx m_R$. The heavier m_R, the lighter m_ν which is why this mass-generating scheme is called seesaw-mechanism. For a more detailed derivation, see [15, 16].

Since neutrinos are only charged under the weak interaction and only LH neutrinos can interact weakly, the RH neutrino is completely sterile under all SM interactions. This has the nice effect, that the sterile neutrino's mass is not restricted to the Electroweak scale (which is used in the seesaw mechanism where $M \sim \mathcal{O}(10^{15})$ GeV is assumed). On the other hand, what hope do we have to find a particle that is non-interacting? The answer to that question is mixing.

2.2 Mixing between active and sterile states

Neutrinos mix because their flavor (or interaction) eigenstates are different from their mass (or propagation) eigenstates [17, 18]. The flavor states α can be expressed as a combination of the mass eigenstates i:

$$|\nu_\alpha\rangle = \sum_i U_{\alpha i}^* |\nu_i\rangle, \tag{2.7}$$

where in the standard three-flavor framework $U_{\alpha i}$ is the 3×3 Pontecorvo–Maki–Nakagawa–Sakata (PMNS) matrix containing three mixing angles θ_{ij} and one CP-violating phase δ_{CP}, $\alpha = \{e, \mu, \tau\}$, $i, j = \{1, 2, 3\}$. If the masses of the neutrinos ν_i are different, their relative phases will change as they propagate through the vacuum. This leads to neu-

trino oscillations. In the two-generation picture first described by Maki, Nakagawa and Sakata in 1962 [19], the mixing is greatly simplified to

$$\begin{pmatrix} \nu_\alpha \\ \nu_\beta \end{pmatrix} = \begin{pmatrix} \cos\theta_{12} & \sin\theta_{12} \\ -\sin\theta_{12} & \cos\theta_{12} \end{pmatrix} \begin{pmatrix} \nu_1 \\ \nu_2 \end{pmatrix} \tag{2.8}$$

with one mixing angle as the only parameter. The relative phase of the propagating mass eigenstates ν_1 and ν_2 is $\Delta\phi(l) = E_1 - E_2 = \frac{\Delta m^2}{2E} l$ with $\Delta m^2 = m_2^2 - m_1^2$. The probability to measure a neutrino of flavor β at a distance l (or equivalently, at time t) which was produced as an α-flavor neutrino at $t = l = 0$ is then:

$$P_{\nu_\alpha \to \nu_\beta} = 1 - \langle \nu_\alpha(l) | \nu_\alpha(0) \rangle = \sin^2 2\theta_{12} \sin^2 \left(\frac{\Delta m^2}{2E} l \right), \tag{2.9}$$

where $\sin^2 2\theta_{12}$ is the depth of oscillation between states α and β. The length scale of oscillations is given by the oscillation length, $L_{osc} = \frac{2\pi E}{\Delta m^2}$. The length that the two mass eigenstates have to propagate to be in phase again, $\Delta\phi = 2\pi$, then equals twice the oscillation length.

In the general three-flavor picture the description of neutrino oscillations is much more complicated. For this thesis however, the two-state framework will be sufficient.

Right-handed neutrinos are not completely sterile, but can mix with the active neutrinos. The mixing between active and sterile states can be described in the same way as the ordinary mixing in the active sector, where the PMNS matrix from (2.7) is expanded to contain $i = \{1, 2, 3, s_1', s_2', s_3', ...\}$ where the s_i' denotes a mostly sterile mass eigenstate, and $\alpha = \{e, \mu, \tau, s_1, s_2, s_3, ...\}$ with sterile flavor eigenstates s_i. The active states α can then mix with all the sterile states. However, usually it is assumed that one active-sterile mixing parameter U_{as}, parameterized by the vacuum mixing angle $\theta_{as} = \theta$ is much larger than the remaining ones, which are set to zero for simplicity. If the active state is a $\nu_{\alpha,L}$, it would mix with a $\overline{\nu^C_{s,R}}$. With $\theta \sim \frac{m_a}{m_s}$, in analogy to the seesaw case, typical examples of mixing angles in different scenarios are:

$\theta \approx 0$	seesaw mechanism,
$\theta \approx 10^{-4} - 10^{-6}$	keV sterile neutrino,
$\theta \approx 10^{-1}$	eV sterile neutrinos.

The mass of the active neutrinos are unknown, but from oscillation data $\sum \nu_a \gtrsim 0.06$ eV (for normal mass hierarchy with $0 \leq m_1 < m_2 < m_3$) or $\sum \nu_a \gtrsim 0.10$ eV (for inverted mass hierarchy with $0 \leq m_3 < m_1 < m_2$) [17] while from cosmological data $\sum \nu_a <$

0.23 eV [12].

2.3 A brief introduction to extra dimensions

In an early attempt at the unification of fundamental forces, a five-dimensional theory was proposed in 1914 by Nordström [20] to unify the electromagnetic and gravitational field. It was expanded on in the 1920s by Kaluza and Klein [21] showing that a compactified extra dimension would lead to a quantization of the momentum in the direction of the fifth dimension. A particle needs a small wavelength – i.e. a high energy – to probe the compactified extra dimension, and the energy needed is anti-proportional to the radius of compactification, $E \sim nR^{-1}$ with $n \in \mathbb{N}$. In the effect, any particle probing the extra dimension will appear to us as a Kaluza-Klein (KK) tower of states. The theory is also applicable today for Beyond the Standard Model Physics as a high-energy extension to the SM.
Revived for unification purposes many decades later, the theory is applicable today for Beyond the Standard Model Physics as a high-energy extension to the SM. In string theory, extra dimensions can lower the fundamental scale of Grand Unification (GUT) [22]. While there exist a number of extra-dimensional models, they can roughly be divided into two groups: universal and non-universal extra dimensions. In the universal extra dimensions (UED) case lowering the GUT scale down to the electroweak scale, all particles with high enough energies can probe the extra dimension and exist with the corresponding tower of states. Since these models are therefore testable at accelerators, quite stringent bounds exist on the sizes of the extra dimensions. A different aproach is the group of non-universal extra-dimensions models, where the SM particles are confined to our ordinary four-dimensional manifold, called a brane, which is embedded in a higher-dimensional bulk. The ADD model [6] is such a model with compactified extra dimensions of rather simple geometry. It was originally proposed to explain why the electroweak scale, $m_{EW} \sim 10^3$ GeV, and the Planck mass (where gravity becomes strong), $M_{Pl} \sim 10^{18}$ GeV are so many orders of magnitude apart. The main idea is that while gravitons, the excitations of the gravity field, freely propagate through the so-called bulk with $n \geq 2$ extra dimensions, the other fields do not. Gravity is then observed to be so weak, because it is spread out over more dimensions. The gravitational potential between two masses m_1, m_2 a distance $|r|$ apart in a theory with compactified

extra dimensions is

$$\Phi(|r|) = \begin{cases} \frac{m_1 m_2}{M_*^{2+n}} \frac{1}{|r|^{n+1}}, & |r| \ll R \\ \\ \frac{m_1 m_2}{M_*^{2+n} R^n} \frac{1}{|r|}, & |r| \gg R. \end{cases} \tag{2.10}$$

One can then lower the Planck scale to the electroweak scale by requiring

$$M_{Pl}^2 \sim M_*^{2+n} R^n \tag{2.11}$$

where M_{Pl} is the effective four dimensional Planck mass, and $M_* \sim m_{EW}$, so the Planck mass of the full $4+n$-dimensional theory and the electroweak mass are about the same. Then, the only fundamental scale is the electroweak one. For only one extra dimension, however, the radius needed to satisfy (2.11) is $R_{n=1} \sim 10^{11}$ m. Obviously this is excluded as it would have noticeable effects on e.g. the planetary orbits in the solar system. For two or more extra dimensions, the radii are at the sub-millimeter scale, which gravitational measurements cannot yet probe. The extra-dimensional setting was first applied to neutrinos with RH neutrinos propagating in the bulk in [23], where the authors explained the small mass of the active neutrinos by a higher-dimensional see-saw mechanism.

So far, no deviations from Newtonian gravity consistent with the presence of ED have been observed. One of the constraints of any extra-dimensional model therefore is, that the laws of gravity be unchanged, i.e. the gravitational potential is inversely proportional to the distance from its source, $\Phi \propto 1/|r|$, at any scale presently accessible by measurement. Therefore, any additional spatial dimension needs to be compactified to a smaller scale than presently measurable. For only one extra dimension, the radius is required to be $R \leq 44\,\mu$m [24] from gravitational inverse-square law tests and $R^{-1} > \mathcal{O}(\text{TeV})$ from graviton searches. For two flat compactified non-universal extra dimensions, the present constraint for their compactification radius is $R \lesssim 30\,\mu$m [25]. Note that in natural units $1\text{eV}^{-1} \approx 0.2\,\mu$m holds.

Since any measurement we make is confined to four dimensions, we see the momentum along the extra dimension as a part of the particle's mass: $m_0^2 + p_y^2 = E^2 - \mathbf{p}^2$.

2.4 Neutrinos and mixing in extra dimensions

We work in an effective five-dimensional model, where only one of several extra spatial dimensions is "large", and the radius of this extra dimension of interest is R. We assume that only sterile neutrinos and gravity can probe this LED, while the other smaller di-

mensions remain hidden to sterile neutrinos.
Since we are considering one effective ED, we can compactify it on an S^1/Z_2 orbifold: a circle S^1 with radius R where any field f is quantized in y direction: $f(y) = f(y + 2\pi R)$ with the Z_2 transformation $y \to -y$. We will take y as the coordinate of the LED and x for the four ordinary dimensions.

2.4.1 Neutrino fields and mass terms

We now intrioduce one SM singlet fermion Ψ. As a singlet it is not restricted to the four-dimensional brane, but can propagate in the bulk. The action is [26]:

$$S = \int \mathrm{d}^4x\mathrm{d}y \left(i\overline{\Psi}\not{\partial}\Psi - 1/2\left(\overline{\Psi^c}M_0\Psi + h.c.\right)\right) \tag{2.12}$$

$$+ \int_{y=0} \mathrm{d}^4x \frac{1}{\sqrt{M_{ED}}} \left(-\overline{\nu_L}\hat{m}^c\Psi - \overline{\nu_L^c}\hat{m}\Psi + h.c.\right), \tag{2.13}$$

where M_{ED} is the mass scale of the higher-dimensional theory, defined as $2\pi R M_{ED} = (M_{Pl}/M_*)^2$. The first integral in (2.13) gives the relevant part of the bulk action, and the second integral gives the brane-bulk coupling. Note that Majorana mass terms are not allowed in five-dimensional spacetime, however $\overline{\Psi^c}M_0\Psi$ leads to an effective Majorana mass term in four dimensions. We will set $M_0 = 0$ for simplicity, noting that one can always rearrange the resulting mass matrix such that a non-zero Majorana mass M_0 has no impact on the mixing scheme. For further details, see [23].
In the four-dimensional case, the fermion field can be decomposed into two two-dimensional Weyl-spinors, $\psi = (\psi_L, \psi_R)$. In five dimensions, we can decompose the singlet into two four-dimensional Weyl spinors ξ and η: $\Psi^T = (\xi, \eta^c)$ with $\eta^c = i\sigma_2\eta^*$ and require ξ to be even and η to be odd under $y \to -y$. Fourier expanding the field along y, we obtain

$$\Psi(x,y) = \frac{1}{\sqrt{\pi R}} \sum_{k=-\infty}^{\infty} \Psi_k(x) e^{iky/R} \tag{2.14}$$

$$= \frac{1}{\sqrt{\pi R}} \left[\xi_0 + \sqrt{2}\sum_{k=1}^{\infty}\left(\xi_k(x)\cos\frac{ky}{R} + \eta_k(x)\sin\frac{ky}{R}\right)\right], \tag{2.15}$$

where we have identified $\xi_0 = \Psi_0$, $\xi_k = \frac{1}{\sqrt{2}}(\Psi_{+k} + \Psi_{-k})$ and $\eta_k = \frac{i}{\sqrt{2}}(\Psi_{+k} - \Psi_{-k})$. This is the KK-expansion of the fermion field Ψ in an effective five-dimensional spacetime with the fifth dimension compactified to an S^1/Z_2-orbifold. After integrating over dy

the action reads:

$$S = \int \mathrm{d}^4x \left[\xi_0^* i\bar{\sigma}^\mu \partial_\mu \xi_0 + \sum_{k=1}^{\infty} \left(\xi_k^* i\bar{\sigma}^\mu \partial_\mu \xi_k + \eta_k^* i\bar{\sigma}^\mu \partial_\mu \eta_k \right) \right. \tag{2.16}$$

$$- \frac{1}{2} \sum_{k=1}^{\infty} \left(\frac{k}{R} \overline{\xi_k^c} \xi_k - \frac{k}{R} \overline{\eta_k^c} \eta_k + h.c. \right) \tag{2.17}$$

$$\left. - \left(\overline{\nu_L^c} m_D \xi_0 + \sqrt{2} \sum_{k=1}^{\infty} \overline{\nu_L^c} m_D \xi_k \right) \right], \tag{2.18}$$

where $\bar{\sigma}^\mu = (1, \boldsymbol{\sigma}_i)$ with the Pauli matrices σ_i. In the basis $(\nu_L, \xi_0, \xi_1, \eta_1, \xi_2, \eta_2, ...)$ the mass matrix then reads:

$$\mathcal{M} = \begin{pmatrix} 0 & m_D & \sqrt{2}m_D & 0 & \sqrt{2}m_D & 0 & \dots \\ m_D^T & 0 & 0 & 0 & 0 & 0 & \dots \\ \sqrt{2}m_D^T & 0 & 0 & 1/R & 0 & 0 & \dots \\ 0 & 0 & 1/R & 0 & 0 & 0 & \dots \\ \sqrt{2}m_D^T & 0 & 0 & 0 & 0 & 2/R & \dots \\ 0 & 0 & 0 & 0 & 2/R & 0 & \dots \\ \vdots & \vdots & \vdots & \vdots & \vdots & \vdots & \ddots \end{pmatrix}. \tag{2.19}$$

The zero-mode ξ_0 corresponds to the RH part of the active neutrino which forms a Dirac pair $\nu_\alpha = (\nu_L, \xi_0^c)$, and the heavier KK modes form Dirac pairs $\nu_{s,k} = (\eta_k, \xi_k^c)$. We can then rewrite the neutrino mass term from (2.18) as

$$\overline{\mathcal{N}_L} \begin{pmatrix} m_D & \mathbf{\sqrt{2}m_D} \\ 0 & M_{KK} \end{pmatrix} \mathcal{N}_R \tag{2.20}$$

where $\mathcal{N} = (\nu_\alpha, \nu_{s1}, \nu_{s2}, ...)$, $\mathbf{\sqrt{2}m_D}$ denotes a vector entry and the mass matrix for the KK modes is

$$M_{KK} = \mathrm{diag}(1/R, 2/R, 3/R, ...). \tag{2.21}$$

2.4.2 Neutrino mixing

Even though we only introduced one RH neutrino field Ψ, it splits up in an infinite tower of states with ever increasing mass as an effect of propagating through the extra dimension. Assume now, that this field Ψ only mixes with one active state, say ν_α and

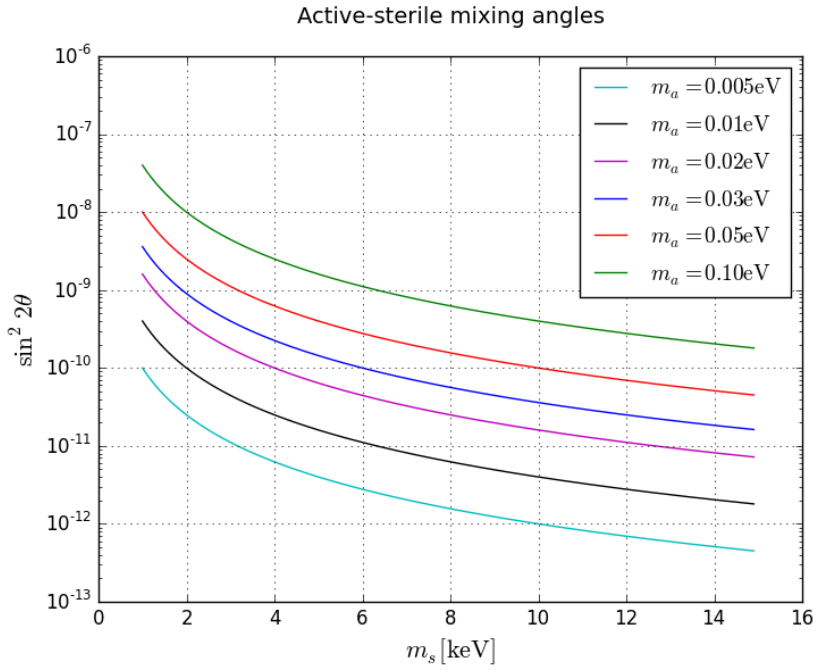

Figure 2.1: The active-sterile mixing angle $\sin^2 2\theta$ as a function of the sterile neutrino mass m_s for different values of the active mass m_a.

does not mix with the remaining active states ν_β. Then, like above, we can write

$$|\nu_\alpha\rangle = \sum_i U^*_{\alpha i}|\nu_i\rangle,$$

where the neutrino content is extended from the standard three mass eigenstates $i = \{1, 2, 3\}$ to include an arbitrary number of sterile states as well: $i = \{1, 2, 3, s1, s2, s3, ...\}$. We want to remark that if we allow each active neutrino state to have its own accompanying tower of sterile neutrinos probing the extra dimension, the description would not change. As the active neutrino mass is very small, much smaller than the mass of the first sterile mode, the sterile states would be degenerate and in fact indistinguishable. As the admixtures of each active state would thus be unresolved, we can redefine the mixing and work with one effective active-sterile mixing angle.
The mixing is then given by $U\text{diag}(m_i)M_{KK}^{-1}$, so that the mixing angles between the α and sk states are approximately $\theta_{\alpha,sk} \sim \frac{m_a}{m_{sk}} = \frac{m_a}{k/R} \propto 1/k$ where k denotes k^{th} excited KK mode of the sterile neutrino. From now on, we will refer to $\theta_{\alpha,sk}$ simply as θ_k. An example of active-sterile mixing angles is given in Figure 2.1.

From (2.21) one can see that a four-dimensional mass of the KK modes of

$$m = \sqrt{m_0^2 + m_{sk}^2} \approx k/R \tag{2.22}$$

is measured, where m_0 is the mass of the zeroth mode, or, the mass of the active neutrino. We can see that the mass of the excited modes and their mixing to active states only depend on the radius on the LED. Furthermore, the ratios of masses and mixing (for subsequent states) are fully determined. In this model, one therefore cannot set mixing between the active neutrino and higher sterile modes to zero a priori, but has to take a infinite number of states and their mixing into account. On the other hand, the mixing is a strictly determined function of the mode number k, and mixing to higher states is suppressed more strongly. Thus we can assume that there exists some yet to be determined mode number $k_{\max}$, for which the mixing is suppressed too much to be of significance.

To give an example, a sterile neutrino with $k = 1$, $m_{s1} = 7.1$ keV mixing with an active neutrino of mass $m_a = 0.03$ eV then comes with a tower of states with masses and corresponding mixing angles

$$m_{sk} = (7.1, 14.2, 21.3, ...)\,\text{keV} \tag{2.23}$$

$$\sin^2 2\theta_k = (7, 1.75, 0.78, ...)\,10^{-11} \tag{2.24}$$

and corresponds to a size of the LED of $R = 0.03$ nm.

In the following we will study production mechanisms for sterile neutrino WDM in the Early Universe.

Chapter 3

Sterile neutrino Dark Matter production mechanisms

In this chapter, we will investigate ways of generating the right sterile neutrino abundance in the Early Universe to account for the DM. The DM abundance, as measured recently by the Planck satellite, amounts to [12]

$$\Omega_{DM}h^2 = 0.1199 \pm 0.0027. \tag{3.1}$$

Throughout this chapter we will assume that only one active neutrino flavor, which we call ν_α mixes with the (one) sterile neutrino flavor, called ν_s. We will use indices s and α to indicate ν_s, and ν_α, respectively. There are various models and scenarios which can be used to generate sterile neutrinos in the keV-mass range, e.g. the Frogatt-Nielsen mechanism with [27] or without [28] an additional flavor symmertry, split seesaw [29], extended seesaw [30] and more (for an overview, see [31]). Our approach to generate sterile neutrino DM closely follows the work by Shi and Fuller [32]. Note that for the temperatures considered here ($\lesssim$ 200 MeV), the calculations are valid for $\alpha = e, \mu$ if $T \lesssim 180$ MeV, and for $\alpha = e, \mu, \tau$ for $T \gtrsim 180$ MeV, as τ are significantly populated only for $T \gtrsim 180$ MeV, while μ are significantly populated at $T \gtrsim 20$ MeV [33]. At a temperature in the early universe of $T_{\rm QCD} \approx 200$ MeV, the quark-hadron phase transition took place, drastically reducing the number of degrees of freedom. Therefore, all sterile neutrino abundance produced before $T_{\rm QCD}$ would have been diluted and is not likely to significantly contribute to the overall DM abundance.

To be a good WDM candidate, the sterile neutrino should be in the mass range of $\approx 2 - 10$ keV. Masses below 2 keV are in tension with bounds from Lyman-α observations

[34, 35, 36] and newer results based on $z > 4$ quasar spectra [37] even suggest $m \gtrsim 3.3$ keV for a thermal WDM particle. These observations of Lyman-α absorption lines in the spectra of distant quasars can be used to determine the time of reionization. This in turn can be translated to a time at which larger structures must have had formed, or, at which DM particles should have been non-relativistic, placing a lower bound on the mass of WDM particles at $\sim 1.7 - 2$ keV. Masses above 10 keV are constrained by diffuse X-ray observations. Also, as the mass goes up, the mixing angle with active neutrinos goes down, which makes production of the correct abundance more difficult in the scenario presented here.

3.1 Non-resonant production

If the masses of the sterile neutrinos are in the keV range, their mixing to the active sector must be very small, as larger mixing is severely constrained by various bounds (see Figure 3.1). Therefore, the easiest way of production by non-resonant oscillation, the Dodelson–Widrow (DW) mechanism [38], does not yield a sufficient sterile neutrino abundance.

The DW mechanism assumes a production of sterile neutrinos via oscillation from an active neutrino species. Because of non-zero mixing, an abundance of sterile neutrinos builds up in the Early Universe, corresponding to an equilibrium fraction of sterile-to-active neutrinos. The sterile neutrinos are produced at plasma temperatures of GeV $> T >$ MeV, before active neutrinos freeze out. Therefore, the sterile neutrinos have a thermal Fermi-Dirac distribution just like the active ones. The DW mechanism accounts for an energy density of [34]

$$\Omega_s^{DW} \approx 0.2 \left(\frac{\sin^2 \theta}{3 \cdot 10^{-9}} \right) \left(\frac{m_s}{3\text{keV}} \right)^{1.8}, \tag{3.2}$$

which can be rewritten as

$$\Omega_s^{DW} h^2 \approx 0.09 \left(\frac{\sin^2 2\theta}{12 \cdot 10^{-9}} \right) \left(\frac{m_s}{3\,\text{keV}} \right)^{1.8} \tag{3.3}$$

using $h = 0.673 \pm 0.012$ [12]. However, this formula is only valid for a narrow mass range of $\approx 1 - 3.4$ keV as will become clear soon. (3.3) was derived comparing the abundance of sterile neutrinos to the abundance of active neutrinos. However, the abundance of a species is related to the effective number of degrees of freedom g_* at the time when the

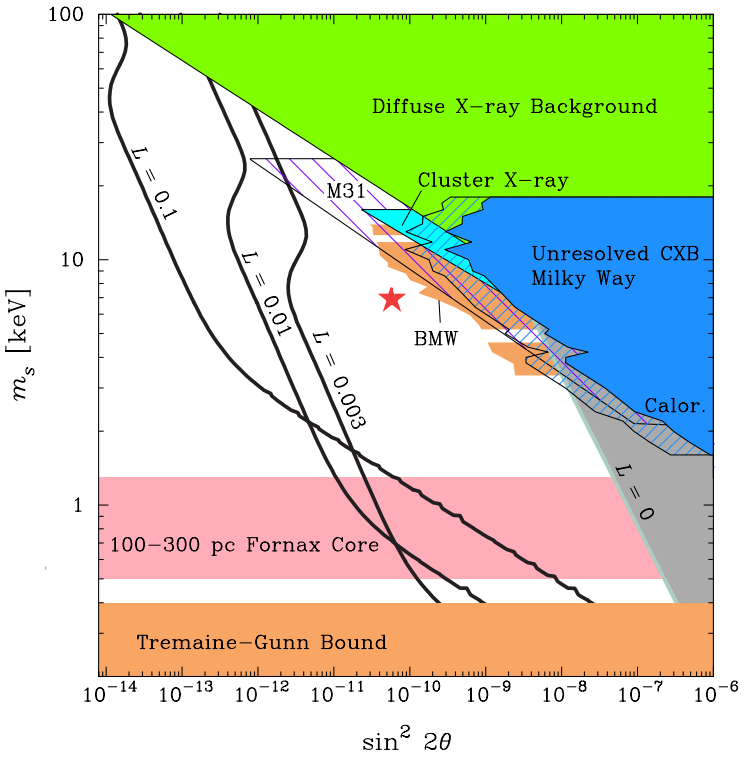

Figure 3.1: Allowed and excluded regions of sterile neutrino WDM parameter space, the star marking the sterile neutrino ($m_s = 7.1$keV, $\sin^2 2\theta \approx 7 \cdot 10^{-11}$) consistent with the recent claim. The white region marks the allowed parameter space, all other colored regions are excluded by various observations, or by phase-space-considerations (orange) or by various observations (green: diffuse X-ray background; blue, light-blue and striped purple: X-ray observations of the Milky Way, clusters and M31 respectively). The pink region is favored to explain the core in the Fornax dwarf, but excluded by Lyman-α observations. L denotes the lepton number; the gray $L = 0$ line corresponds to the Dodelson-Widrow mechanism, which in the grey solid region leads to overproduction. Taken from [5].

species freezes out g_{*f} [39]:

$$\Omega h^2 = 7.83 \cdot 10^{-2} \frac{g_{*f}}{g_{\text{eff}}} \tag{3.4}$$

where for a two-component neutrino species $g_{\text{eff}} = 1.5$. Therefore, (3.3) is only valid if the number of effective degrees of freedom does not significantly change between the time of production and the freeze-out of active neutrinos. This is the case for sterile neutrinos being produced after the QCD-transition at $T_{\text{QCD}} \approx 200$ MeV. Around T_{QCD}, the number of effective degrees of freedom g_* changes rapidly from $g_* = 106.75$ to $g_* = 10.75$, diluting the already-present sterile neutrino abundance by the dilution factor $\frac{10.75}{g_*(T_{\text{Peak}})}$ [39]. Production of sterile neutrinos with the DW mechanism peaks at temperatures of

$$T_{\text{Peak}} \simeq 133 (m_s/\text{keV})^{1/3} \text{MeV}. \tag{3.5}$$

For $T \gg T_{\text{Peak}}$, the production falls off with T^{-9}, while for $T \ll T_{\text{Peak}}$, it is $\propto T^3$, so that most of the abundance is produced close to T_{Peak} [38].

For a 7.1 keV sterile neutrino with a vacuum mixing angle of $\sin^2 2\theta = 7 \cdot 10^{-11}$, the production via the DW mechanism peaks at $T_{\text{Peak}} \simeq 256$ MeV, so that the abundance amounts to

$$\Omega_s^{DW}(m_s = 7\,\text{keV}) h^2 \approx 0.0025 \frac{10.75}{g_*(T_{\text{Peak}})} = 0.00025, \tag{3.6}$$

or, 0.2 % of the dark matter content of the universe. Even an extreme (and ruled out) value of $m_s = 1$ keV, $m_a = 0.1$ eV leads to a density of $\Omega_s^{DW} h^2 \approx 0.042$, about one third of what is needed. In general, the DW mechanism can generate sterile neutrinos in the right abundance to account for DM in the mass range of $1 - 3$ keV. This, however, is in excluded by Lyman-α observations, as explained above.

To still produce a high enough number of sterile neutrinos in the Early Universe to account for a significant part of the DM, resonant production is assumed via the enhancement of the oscillation in an asymmetric medium with adiabatic flavor conversion, known as the Shi–Fuller (SF) mechanism.

3.2 Resonant production

3.2.1 Neutrino propagation in a dense medium

A particle's propagation properties generally differ from their vaccum values in the presence of a surrounding medium. If the particle is in an asymmetric medium, where there is a surplus of matter (or antimatter), the effect of the dense medium will differ for the particle wrt. its antiparticle. To get the effect the medium has on the particle, one can

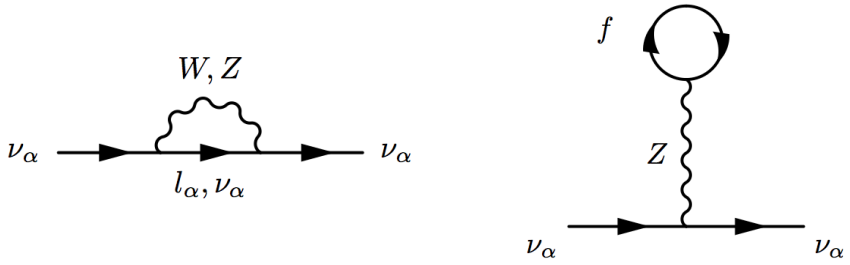

Figure 3.2: One-loop thermal contribution to neutrino self-energy. **Left:** Bubble graph. The fermion in the loop can either be a neutrino of the same flavor ν_α or the corresponding charged lepton. **Right:** Tadpole graph. The fermion in the loop can be any fermion in thermal equilibrium.

calculate the one-loop thermal contribution to the self-energy of that particle, as shown in [40]. The net effect is a changing in the index of refraction for the particle, thus changing its propagation through the medium. For a neutrino of flavor α, the contribution to its self-energy is given by the loop diagrams in Figure 3.2.

We define the asymmetry of a particle χ as the overabundance of χ particles relative to the abundance of photons, $L_\chi = \frac{n_\chi - n_{\overline{\chi}}}{n_\gamma} = \frac{\Delta n_\chi}{n_\gamma}$. We know that for baryons, $L_b \approx 10^{-10}$, and alike for charged leptons (from non-observations of a charge asymmetry in the universe). Thus, we only have to take into account the effects of a lepton asymmetry in the neutrino sector, neglecting any other contribution as it is many orders of magnitude weaker. For a neutrino of flavor α propagating through a medium of neutrinos of the same flavor, both diagrams in Figure 3.2 give a contribution to the neutrino's self-energy: a neutrino of the same flavor can propagate in either of the loops shown in Figure 3.2. In a medium of neutrinos of a different flavor only the tadpole diagram contributes as a fermion of a different flavor can only propagate in the loop shown on the right of Figure 3.2. Now, both diagrams yield the same contribution to the self-energy,

$$\Delta E_{\text{tadpole/bubble}}(\nu_\alpha) = \sqrt{2} G_F \Delta n_{\nu_\alpha} \tag{3.7}$$

where $G_F = 1.166 \cdot 10^{-5}\,\text{GeV}^{-2}$ is the Fermi constant. In the Early Universe the total contribution to the self-energy of an active neutrino from a lepton asymmetric plasma

is:

$$\Delta E_{\text{asym.}}(\nu_\alpha) = \Delta E_{\text{bubble}}(\nu_\alpha) + \Delta E_{\text{tadpole}}(\nu_\alpha) + \sum_{\beta\neq\alpha} \Delta E_{\text{tadpole}}(\nu_\beta) \tag{3.8}$$

$$= \sqrt{2} G_F \left(2 \cdot \Delta n_{\nu_\alpha} + \sum_{\beta\neq\alpha} \Delta n_{\nu_\beta} \right). \tag{3.9}$$

Obviously, the medium has the opposite effect for an antiparticle of the same type: $\Delta E(\overline{\nu}_\alpha) = -\Delta E(\nu_\alpha)$. The effect of the medium on the particle's propagation can be expressed as an additional term in the oscillation potential.
Another term that needs to be taken into account is the thermal contribution coming from a symmetric medium, in which a neutrino can be scattered. Scattering suppresses oscillations, as it destroys a coherent evolution of the phase relation between the active and sterile state. Scattering always leaves a neutrino in a pure active flavor state, and the phase relation between the mass eigenstates is set back to the initial value. The thermal contribution is proportional to the scattering rate and reads [40, 32]:

$$\Delta E_{\text{thermal}} \sim -10^2 G_F^2 E T^4 \tag{3.10}$$

and always acts as a damping term. The thermal contribution also explains why for small mixing angles, the DW mechanism introduced in the previous section yields vanishing contributions: the oscillation lengths are large compared to the scattering rate, and the probability of the active neutrino to oscillate into a sterile state decreases greatly.

3.2.2 The Mikheev–Smirnov–Wolfenstein effect

The Mikheev–Smirnov–Wolfenstein (MSW) effect [41] uses the effect a dense, lepton-asymmetric medium has on neutrino oscillations. It explains why the solar neutrino flux observed with detectors (mostly) sensitive to the electron neutrino flavor was less than the estimated (total) solar neutrino flux, and also why that neutrino "deficit" was energy dependent. The Sun provides a dense, asymmetric medium that changes the index of refraction of a propagating ν_e and therefore changes the length of oscillation into a $\nu_{\mu,\tau}$. For the MSW effect the lepton asymmetry in the electron sector is dominant, as electron neutrinos scatter off electrons, while neutrinos of other flavors do not. This introduces an additional matter oscillation potential. If the matter effect cancels the vacuum oscillation potential, the matter mixing angle becomes maximal, and the oscillation is resonant. In a medium of uniform density, the matter effect can be written in terms of

redefined propagation eigenstates ($\nu_i \to \nu_{im}$) and mixing angles ($\theta \to \theta_m$). The depth of oscillations changes as well ($\sin^2 2\theta \to \sin^2 2\theta_m$) and might be enhanced (or suppressed). Nevertheless, the oscillation process can be described in analogy to vacuum oscillations, i.e. the flavor composition of the neutrino mass eigenstates is different than in vacuum, but fixed. In a medium of varying density, however, the mixing angle depends on the local density and therefore changes during propagation. In effect, the propagation eigenstates are not fixed anymore, but vary with the varying density. If the density varies slowly, the eigenstates can follow adiabatically, and their flavor composition changes. This can lead to a non-oscillatory conversion of flavors. If a ν_e is produced in the solar interior and at production mostly corresponds to a ν_{2m} eigenstate and travels outward through layers of decreasing density, this propagation eigenstate will change accordingly and become the vacuum eigenstate ν_2. As the ν_2 only has a small admixture of ν_e, the neutrino will probably interact as a $\nu_{\mu,\tau}$ once it leaves the sun. Of importance for the conversion is the difference of the admixtures of the flavor states to the propagation state between the production and the interaction point. The flavor conversion mainly happens in a density layer where the oscillation is resonant, an the effective oscillation potential is zero. For neutrinos produced outside the sun and traveling through it, the initial and final conditions are equal and therefore there is no adiabatic flavor conversion. Since the oscillation potential depends on the neutrino's energy, neutrinos of different energies will encounter resonant regions in different layers in the sun, and for some neutrino energies, the resonance condition will not be fulfilled at all. In particular, the MSW adiabatic conversion holds for high-energy neutrinos with $E > 10$ MeV, with a mix of conversion and enhanced oscillations for neutrinos in the range of $E \approx 2 - 10$ MeV.

3.2.3 The Shi–Fuller mechanism

The Shi–Fuller (SF) mechanism is based on the MSW-effect and can be used to produce sterile neutrinos resonantly, if certain conditions in the Early Universe are fulfilled:

- the dense material changes the oscillation parameters: the matter mixing angle $\sin^2 2\theta_m$ is different from the vacuum mixing angle $\sin^2 2\theta$
- there is an asymmetry between neutrinos and antineutrinos which enhances the matter mixing angle and can make it maximal
- the resulting resonance is adiabatic, and thus very effective in converting active to sterile states $\Rightarrow$ essentially all ν_α in the resonant region get transformed into ν_s

In the Early Universe, the medium is nearly symmetric for baryons and charged leptons, but for neutrino asymmetries the current bounds are much more loose. Since the medium has no effect on a sterile neutrino, the difference in energy between the active and the sterile neutrino is the medium contribution to the self-energy of the active neutrino. Following [32], we will do the calculation for an active neutrino. The same result applies for an active antineutrino oscillating into a sterile state if the lepton asymmetry is negative. We identify the lepton-asymmetry term (3.9) $\Delta E_{asym.} := V_\alpha^L$ and the thermal term (3.10) $\Delta E_{thermal} := V_\alpha^T$ as additional terms in the oscillation potential and use $\Delta n_{\nu_\alpha} = \frac{n_{\nu_\alpha} - n_{\overline{\nu}_\alpha}}{n_\gamma} \cdot n_\gamma = \frac{2\zeta(3)}{\pi^2} L_{\nu_\alpha} T^3$. The effective potential of the oscillation between the active and sterile neutrino state can then be written as [32] $\mathbf{V} = (V_x, V_y, V_z)$ where

$$V_x = \frac{\delta m^2}{2E} \sin 2\theta \ , \ V_y = 0 \ , \ V_z = V_0 + V_\alpha^L + V_\alpha^T. \tag{3.11}$$

Here, V_x is the transformation rate, $V_0 = -\frac{\delta m^2}{2E} \cos 2\theta$ is the vacuum oscillation potential given by the mass splitting $\delta m^2 = m_s^2 - m_\alpha^2$ and the mixing angle θ. The contribution from the plasma derived above (3.9) is

$$V_\alpha^L \approx 0.35 G_F T^3 (L_0 + \mathcal{L}), \tag{3.12}$$

with the effective lepton asymmetry

$$\mathcal{L} = 2L_{\nu_\alpha} + \sum_{\beta \neq \alpha} L_{\nu_\beta}. \tag{3.13}$$

The lepton asymmetry in the oscillating neutrino flavor is L_{ν_α} and in the other active neutrino flavors L_{ν_β}. As shown in 3.2.1, the α flavor with mixing with the sterile state contributes twice as much to the effective lepton asymmetry as each flavor β not mixing with the sterile state. $L_0 \sim 10^{-10}$ is the electon-positron and baryon asymmetry, defined above, and can safely be neglected due to its smallness. The thermal neutrino background contributes with $V_\alpha^T \sim -10^2 G_F^2 E T^4$ (3.10) and for the temperatures and lepton asymmetries of interest is a few orders of magnitude smaller than the contribution from the lepton asymmetry. The resonance condition is $V_z = 0$. Neglecting V_α^T and defining the dimensionless spectral parameter $\epsilon = E/T$, we get the resonance temperature

$$\frac{T_{\rm res}}{\rm MeV} \approx 90 \left(\frac{m_s}{\rm keV}\right)^{1/2} \left(\frac{\mathcal{L}}{10^{-3}}\right)^{-1/4} \epsilon_{\rm res}^{-1/4}. \tag{3.14}$$

As the temperature goes down as the universe expands, the resonance sweeps from low to high ϵ and converts the less energetic neutrinos first, yielding a colder-than-thermal distribution of the sterile neutrinos. The resonant conversion is only efficient if it is adiabatic, i.e. if the resonance width moves slowly across the neutrino spectrum. This is equivalent to requiring that the transformation rate times the resonance width being larger than the speed of the resonance:

$$V_x^2 \left|\frac{\mathrm{d}\epsilon_{\mathrm{res}}}{\mathrm{d}V_z}\right| \left|\frac{\mathrm{d}\epsilon_{\mathrm{res}}}{\mathrm{d}t}\right|^{-1} > 1 \tag{3.15}$$

where $|V_x \frac{\mathrm{d}\epsilon_{\mathrm{res}}}{\mathrm{d}V_z}|$ is the energy width of the resonance and $|\frac{\mathrm{d}\epsilon_{\mathrm{res}}}{\mathrm{d}t}|$ is the sweeping speed of the resonance across the neutrino spectrum. With equation (3.11), we find:

$$\frac{\mathrm{d}\epsilon_{\mathrm{res}}}{\mathrm{d}V_z} = \epsilon_{\mathrm{res}}(0.35 G_F T^3 \mathcal{L})^{-1} \tag{3.16}$$

$$\left|V_x \frac{\mathrm{d}\epsilon_{\mathrm{res}}}{\mathrm{d}V_z}\right| \approx \epsilon_{\mathrm{res}} \sin^2 2\theta. \tag{3.17}$$

From equation (3.14), we see that

$$\epsilon_{\mathrm{res}} \approx 90^4 \left(\frac{m_s}{\mathrm{keV}}\right)^2 \left(\frac{\mathcal{L}}{10^{-3}}\right)^{-1} \left(\frac{T_{\mathrm{res}}}{\mathrm{MeV}}\right)^4 \tag{3.18}$$

such that $\mathrm{d}\epsilon_{\mathrm{res}}/\mathrm{d}T = -4\epsilon_{\mathrm{res}}/T$. In the Early Universe [39]

$$T^2 = 0.301 g_*^{-1/2} M_{Pl}/t \tag{3.19}$$

$$H = 1.66 g_*^{1/2} T^2/M_{Pl} \tag{3.20}$$

where $H \approx 5.5T^2/M_{Pl}$ is the Hubble parameter and $M_{Pl} \approx 1.22 \cdot 10^{28}$ eV is the Planck mass. This implies $H = -\dot{T}/T$ where $\dot{T} = \mathrm{d}T/\mathrm{d}t$. The speed of the resonance is due to expansion of the universe and resonant conversion:

$$\frac{\mathrm{d}\epsilon_{\mathrm{res}}}{\mathrm{d}t} = \frac{\mathrm{d}\epsilon_{\mathrm{res}}}{\mathrm{d}T}\frac{\mathrm{d}T}{\mathrm{d}t} + \frac{\mathrm{d}\epsilon_{\mathrm{res}}}{\mathrm{d}\mathcal{L}}\frac{\mathrm{d}\mathcal{L}}{\mathrm{d}t} \tag{3.21}$$

$$= -4\epsilon_{\mathrm{res}}/T \cdot (-HT) - \epsilon_{\mathrm{res}}/\mathcal{L} \cdot \frac{\mathrm{d}\mathcal{L}}{\mathrm{d}t} \tag{3.22}$$

$$= \epsilon_{\mathrm{res}} \left(4H - \frac{\mathrm{d}\mathcal{L}/\mathrm{d}t}{\mathcal{L}}\right). \tag{3.23}$$

This way the adiabaticity condition (3.15) can be rewritten as:

$$4 \cdot 10^8 \left(\frac{m_s}{\text{keV}}\right)^{1/2} \left(\frac{\mathcal{L}}{10^{-3}}\right)^{3/4} \epsilon_{\text{res}}^{-1/4} \sin^2 2\theta \left(1 - \frac{\mathrm{d}\mathcal{L}/\mathrm{d}t}{4H\mathcal{L}}\right)^{-1} \overset{!}{>} 1. \tag{3.24}$$

$\frac{\mathrm{d}\mathcal{L}/\mathrm{d}t}{4H\mathcal{L}}$ is zero when there is no resonant adiabatic conversion (i.e. when conversion stops) and in the extreme case of the slowest possible resonance sweep rate (equalling the Hubble expansion rate) it is 1. The resonance loses adiabaticity at the maximum spectral parameter ϵ_{max}.

In the early universe, we can assume an equilibration of the neutrino lepton asymmetries, $L_{\nu_\alpha} = L_{\nu_\beta}$, due to strong mixing in the dense environment [42], and therefore $\mathcal{L} = 4L_{\nu_\alpha}$. From (3.13) it follows that the change in the effective lepton asymmetry is twice the change in the lepton asymmetry of the α flavor: $\Delta\mathcal{L} = 2\Delta L_{\nu_\alpha}$, if only ν_α can oscillate into the sterile state (and $\Delta L_{\nu_\beta} = 0$). The change in L_{ν_α} can be described by the number of produced sterile neutrinos, or the amount of active neutrinos "lost" due to transformation: $\mathrm{d}L_{\nu_\alpha}/\mathrm{d}t = f(\epsilon)\mathrm{d}\epsilon/\mathrm{d}t$. Then, taking into account that the abundance produced prior to the quark-hadron transition is diluted, $\Delta L_{\nu_\alpha} \approx \int_{\epsilon_{QCD}}^{\epsilon_{\text{max}}} f(\epsilon)\mathrm{d}\epsilon$. The function to integrate is [43]

$$f(\epsilon) = \epsilon^2/(e^{\epsilon-\xi} + 1) \tag{3.25}$$

where ξ is the chemical potential divided by the temperature defined by $L_{\nu_\alpha} = \frac{\pi^2}{12\zeta(3)}(\xi_{\nu_\alpha} + \frac{\xi_{\nu_\alpha}^3}{\pi^2})$, thus $\xi \approx 3/2L_{\nu_\alpha}$. Since the conversion stops at ϵ_{max}, the resulting sterile neutrino spectrum is non-thermal and skewed towards lower energies, i.e. colder than a thermal spectrum, as the sterile neutrinos do not interact and therefore never equilibrate.

As the abundance of an active neutrino is $\Omega_\alpha^{SF}h^2 = \left(\frac{m_a}{91.5eV}\right)$, the sterile neutrino abundance produced via the SF mechanism is given by [32]:

$$\Omega_s^{SF}h^2 = F\left(\frac{m_s}{91.5eV}\right) \tag{3.26}$$

where F is the sterile neutrino number density as a fraction of the number density of the active neutrino. Using the lepton asymmetry L_{ν_α}, $\Delta L_{\nu_\alpha} = \frac{n_{\nu_s}}{n_{\nu_\gamma}}$, and the neutrino number per species before neutrino decoupling being [44] $n_{\nu_\alpha} = \frac{3}{8}n_{\nu_\gamma}$, we find

$$F = \frac{n_{\nu_s}}{n_{\nu_\alpha} + n_{\nu_{\overline{\alpha}}}} = \frac{4}{3}\Delta L_{\nu_\alpha}. \tag{3.27}$$

Thus

$$\Omega_s^{SF}h^2 = 0.0146\frac{\Delta L_{\nu_\alpha}}{10^{-3}}\frac{m_s}{\text{keV}} \tag{3.28}$$

for the sterile neutrino abundance today, produced with the SF mechanism. We see that the abundance only depends on the mass of the sterile neutrino and the transformed lepton asymmetry, which in turn depends on the adiabaticity of the resonance.
We propose to treat $\mathcal{L}$ as a free parameter, and solve the adiabaticity equation for the stop of the adiabatic transformation. We set the adiabaticity equation to 1, and solve for $\mathcal{L}^f$, then $\mathcal{L}^i = \mathcal{L}^f + 2\Delta L_{\nu_\alpha}$ where i and f denote initial and final values, respectively. The constraints for $\mathcal{L}$ are rather lose: $\mathcal{L} \lesssim \mathcal{O}(10^{-2})$ [33, 42] if lepton asymmetries are equal in all flavors. Unlike the authors originally proposing the mechanism, we find that the adiabaticity condition is lost at finite $\mathcal{L}$, therefore $\mathcal{L}$ does not go to zero. This can be easily explained by looking at the adiabaticity condition (3.24). It is proportional to $m_s^{1/2} \sin^2 2\theta \, \mathcal{L}^{3/4} \propto m_s^{-3/2} \mathcal{L}^{3/4}$. Therefore, as the mass of the sterile neutrino increases, the effective lepton asymmetry needs to increase appropriately for adiabaticity to be satisfied. This explains why adiabaticity is lost at higher $\mathcal{L}$ when looking at keV-mass sterile neutrinos as compared to masses of around 100 eV as the authors of [32] originally proposed. Following the resonance, the lepton asymmetries in the different flavors do not equilibrate straight away. This has to be kept in mind when looking at multiple resonances and whether they happen simutaneously or are separated in time.

What happens after adiabaticity is lost?

The conversion mechanism ceases to be efficient after the adiabaticity condition (3.24) is violated. The conversion quickly drops off after the resonance enters the non-adiabatic regime. Therefore non-adiabatic conversion only marginally contributes to the final abundance and we will neglect it in the following. As adiabaticity is lost at non-zero $\mathcal{L}$, the residual lepton asymmetry may drive another resonance for lower mode numbers. This possibility will be investigated in the next chapter.

Chapter 4

Production of sterile neutrino Dark Matter in extra dimensions

4.1 Producing abundances of sterile neutrino modes

After having described the production mechanism, we will now apply the DW and the SF mechanisms to produce a tower of sterile neutrinos. We will study how the presence of the LED influences sterile neutrino abundance, and for what range of masses and mixing angles sterile neutrinos are viable DM candidates. We will start by producing one state, let it be the lightest one, and then see what changes by introducing more modes. For the remainder of the chapter, we will require the sterile neutrino abundance to be equal to the measured DM abundance as given by (3.1).
For all masses and mixing angles of interest, the DW mechanism does not suffice to produce a high enough abundance of sterile neutrinos to account for the DM. Thus, the resonant SF mechanism is responsible for the majority of the sterile neutrino abundance.

4.1.1 The trivial case: one mode

In order to produce one KK mode only, we obviously do not need the extra-dimensional setting. We will still carry out the calculation. This way, we will be able to investigate what actually changes in the presence of a tower of sterile neutrinos. Setting the total sterile neutrino abundance today to the Dark Matter abundance, $\Omega_s h^2 = \Omega_{DM} h^2$ and

keeping in mind that both the DW and the SF mechanism contribute, we can write:

$$\Omega_s^{SF} h^2 = \Omega_{DM} h^2 - \Omega_s^{DW} h^2 \tag{4.1}$$

$$= 0.0146 \frac{\Delta L_{\nu_\alpha}}{10^{-3}} \frac{m_s}{\text{keV}} \tag{4.2}$$

and since $\Delta L_{\nu_\alpha} = \int_{\epsilon_{\text{QCD}}}^{\epsilon_{\max}} f(\epsilon) \mathrm{d}\epsilon$, we finally arrive at:

$$\int_{\epsilon_{\text{QCD}}}^{\epsilon_{\max}} f(\epsilon) \mathrm{d}\epsilon = \frac{\Omega_{DM} h^2 - \Omega_s^{DW} h^2}{0.0146 m_s/\text{keV}} \cdot 10^{-3}. \tag{4.3}$$

Setting the QCD transition as the lower bound of the integral and setting the adiabaticity equation (3.24) to one for the upper bound (both as a function of $\mathcal{L}$), we can solve the integral for $\epsilon_{\max}$.

One interesting example is the case of a sterile neutrino with a mass of 7.1 keV, which was recently proposed as an explanation of a weak, unidentified spectral line observed by [4, 5]. The authors of [5] quote a value of $\sin^2 2\theta \approx 7 \cdot 10^{-11}$ (without stating errors), the authors of [4] give a value of $\sin^2 2\theta = (2.2 - 20) \cdot 10^{-11}$; those mixing angles lie outside the presently excluded region (see 3.1). Obviously an interesting question is whether such a sterile neutrino can be produced with the mechanism introduced above. The result can be seen in Figure 4.1. We can see that most of the suggested parameter space is consistent with the production mechanism introduced, while the higher end of the mixing angle space quoted in [4] may be in tension with constraints to the lepton asymmetry. We are taking into account non-resonant as well as resonant oscillation, even though the non-resonant contribution is completely negligible for this example of sterile mass and mixing angles.

For a lighter sterile neutrino, a larger fraction of active neutrinos needs to get adiabatically transformed to obtain the same abundance. At the same time, the adiabaticity condition is easier to satisfy. Analogously for a heavier neutrino, the fraction that needs to be converted is lower, but adiabaticity might be hard to obtain. Figures 4.2 and 4.3 show the cases for a sterile neutrino with a mass of $m_s = 3.0$ keV and $m_s = 10.0$ keV respectively. One can see how for a lower mass state, a higher amount of active neutrinos needs to be transformed, and the mixing angles need to be marginally larger. For a higher mass state, the required mixing angles have to be slightly lower, and a lower change in lepton asymmetry is needed.

Now one could naively think that the more massive the sterile neutrino, the easier it is to produce with the Shi–Fuller mechanism. This is only true if one leaves the mix-

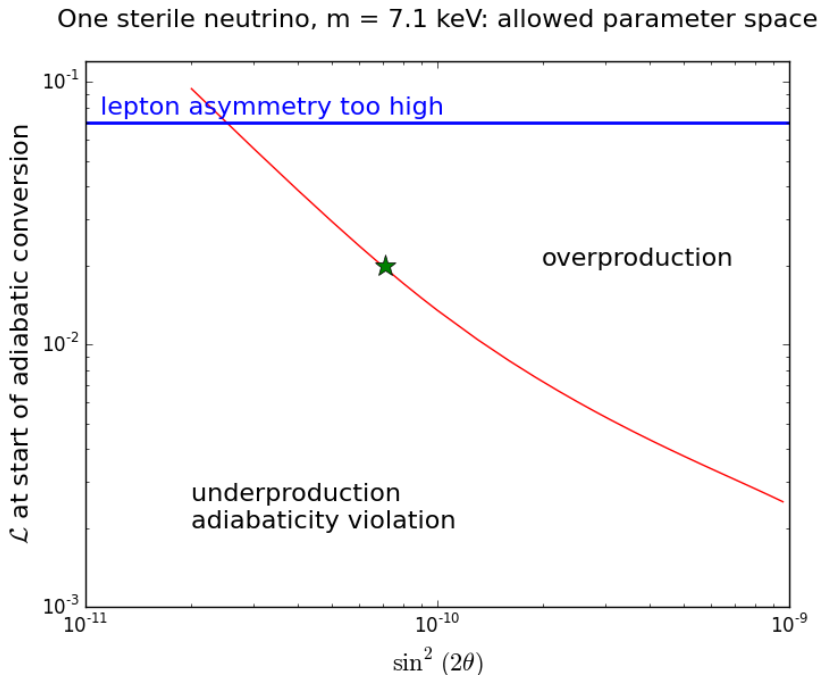

Figure 4.1: $\mathcal{L}$ vs. mixing angle for one 7.1 keV sterile neutrino. The red line shows the parameter space for a correct DM abundance, everything above the blue line is constrained by the maximum value of the lepton asymmetry $\mathcal{L}$. Below the red line the adiabaticity is lost before the correct abundance is obtained, above the red line the conversion goes on for too long (leading to overabundance). The claim by [5] is shown as a green star, the region quoted in [4] extends down to $\sin^2 2\theta = 2 \cdot 10^{-10}$. The required change in lepton asymmetry ΔL_{ν_α} ranges from $0.83 \cdot 10^{-3}$ for $\sin^2 2\theta = 1 \cdot 10^{-9}$ to $1.15 \cdot 10^{-3}$ for $\sin^2 2\theta = 2 \cdot 10^{-11}$.

ing angle unchanged. However, since the mixing angle $\sin^2 2\theta \propto m_s^{-2}$, this argument is quite unphysical. Indeed, comparing Figures 4.1, 4.2 and 4.3, one can see that the mixing angles for when an adiabatic production is possible, do not vary that much (from $\sin^2 2\theta \approx 3 \cdot 10^{-10}$ for $m_s = 3$ keV to $\sin^2 2\theta \approx 1.2 \cdot 10^{-10}$ for $m_s = 10$ keV). However, imagine all of those states having arisen from the same tower of KK modes (and disregard that the mode number is an integer for this example). Taking the star in Figure 4.1 with $m_s = 7.1$ keV and $\sin^2 2\theta \approx 7 \cdot 10^{-11}$ as a reference point leads to a mixing angle of $\sin^2 2\theta \approx 3.8 \cdot 10^{-10}$ for $m_s = 3$ keV and $\sin^2 2\theta \approx 3.4 \cdot 10^{-11}$ for $m_s = 10$ keV. And now we see that the lighter sterile neutrino can be produced adiabatically in this example, while the heavier ones cannot. This will have important implications when looking at multi-state sterile neutrinos: the lower states will be produced much more easily than

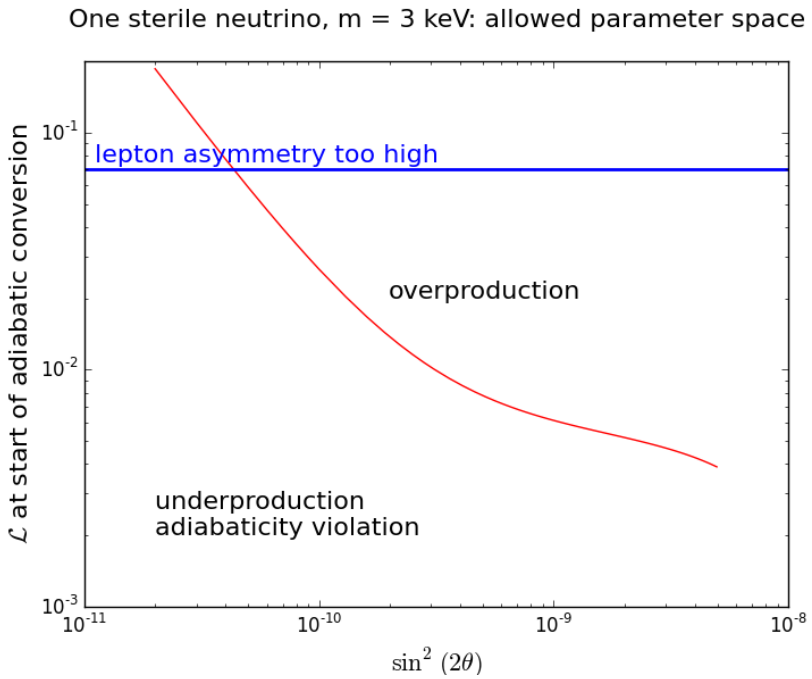

Figure 4.2: $\mathcal{L}$ vs. mixing angle for one 3.0 keV sterile neutrino. The effect of the non-resonant production is visible for larger mixing angles. The required change in lepton asymmetry ΔL_{ν_α} ranges from $1.9 \cdot 10^{-3}$ for $\sin^2 2\theta = 5 \cdot 10^{-9}$ to $2.7 \cdot 10^{-3}$ for $\sin^2 2\theta = 2 \cdot 10^{-11}$.

the higher states.

4.1.2 Adding a second mode

Let us examine what happens if we allow a second KK mode to be present. Of course, there would be arbitrarily many modes that need to be taken into account, but let us now focus on the question how a second mode influences the sterile neutrino DM abundance. From Chapter 2 we know that the mass of a k-th mode goes as $m_{sk} \propto k$ while the mixing angle $\sin^2 2\theta_k \approx 4\theta_k^2 \approx 4(m_a/m_{sk})^2 \propto k^{-2}$. Therefore, $m_{s2} = 2m_{s1}$ and $\sin^2 2\theta_2 = 0.25 \sin^2 2\theta_1$.
From equation (3.18) we can get the spectral parameter:

$$\epsilon_{\text{res}} = 90^4 m_s^2 \left(\frac{\mathcal{L}}{10^{-3}}\right)^{-1} T_{\text{res}}^{-4} \tag{4.4}$$

where T is in MeV and m_s in keV. Since all initially produced sterile neutrino abundance would get diluted by the QCD-transition at around 200 MeV, the vast majority

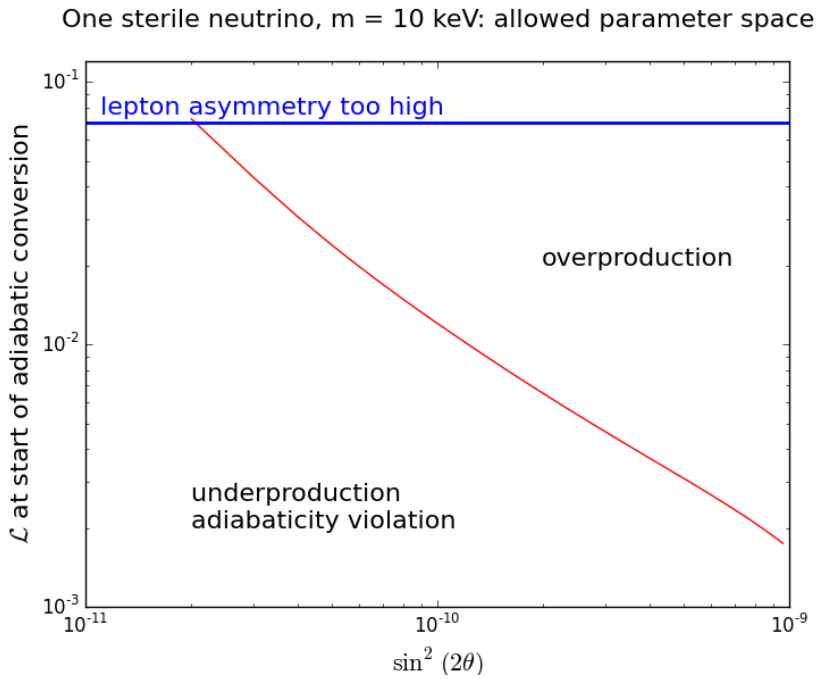

Figure 4.3: $\mathcal{L}$ vs. mixing angle for one 10.0 keV sterile neutrino. The required change in lepton asymmetry ΔL_{ν_α} ranges from $0.39 \cdot 10^{-3}$ for $\sin^2 2\theta = 1 \cdot 10^{-9}$ to $0.81 \cdot 10^{-3}$ for $\sin^2 2\theta = 2 \cdot 10^{-11}$. For higher masses, less active neutrinos need to be transformed into sterile ones, but generally, the mixing angle goes down quadratically with rising mass, so adiabaticity will hold only for larger lepton asymmetries.

of the abundance produced by the SF-mechanism has to come from active neutrinos transforming to sterile neutrinos afterwards, and we set $T = 200$ MeV as the starting value. Then we can rewrite the equation above as

$$\epsilon_{\mathrm{QCD}} = 0.45^4 m_s^2 \left(\frac{\mathcal{L}^i}{10^{-3}} \right)^{-1} . \tag{4.5}$$

The lepton asymmetry transforming active into sterile neutrinos is the same for each mode, since we have assumed that only one active flavor mixes with the KK tower. Thus, since T is really a measure of time, we see that for any time $t = t(T)$

$$\epsilon_{\mathrm{res2}}(t) = 4\epsilon_{\mathrm{res1}}(t) \tag{4.6}$$

and in particular,

$$\epsilon_{\mathrm{QCD2}} = 4\epsilon_{\mathrm{QCD1}} . \tag{4.7}$$

This, of course is consistent with our finding before, that the resonance moves across the active neutrino spectrum from lower to higher spectral parameter and that this movement happens faster for higher sterile masses. This again implies, that the highest state that gets produced adiabatically, will be produced earliest. In case of two resonantly produced states, this would mean that the abundance of the heavier state comes from the integral $\int_{\epsilon_{\mathrm{QCD2}}}^{\epsilon_{\mathrm{max2}}} f(\epsilon)\mathrm{d}\epsilon$, where ϵ_{max2} is the value of the spectral parameter when the resonance becomes non-adiabatic for conversion into the second-lightest sterile state. The lighter state lags behind in the resonance sweep. For the values of ϵ, that the heavier state has already swept through, there are essentially no (or very few) active neutrinos left to convert into the lighter sterile state. Therefore, the dominant contribution to the abundance of the lighter state has to come from the integral $\int_{\epsilon_{\mathrm{max2}}}^{\epsilon_{\mathrm{max1}}} f(\epsilon)\mathrm{d}\epsilon$, where ϵ_{max1} is the value of the spectral parameter when the resonance with the lightest mode becomes non-adiabatic. There is little contribution from $\epsilon < \epsilon_{\mathrm{QCD2}}$, since that part was also transformed into the heavier mode, but its abundance was washed out by a factor of ~ 10 during the QCD-transition.
The abundance produced by the SF mechanism for the two states then is:

$$\Omega^{SF}_{s1+s2}h^2 = 0.0146\left(\frac{\Delta L_{\nu_\alpha 2}}{10^{-3}}\frac{m_{s2}}{\mathrm{keV}} + \frac{\Delta L_{\nu_\alpha 1}}{10^{-3}}\frac{m_{s1}}{\mathrm{keV}}\right) \tag{4.8}$$

$$= 0.0146\,\frac{m_{s1}}{\mathrm{keV}}\left(2\frac{\Delta L_{\nu_\alpha 2}}{10^{-3}} + \frac{\Delta L_{\nu_\alpha 1}}{10^{-3}}\right) \tag{4.9}$$

$$= 0.0146\,\frac{m_{s1}}{10^{-3}\mathrm{keV}}\left(2\int_{\epsilon_{\mathrm{QCD2}}}^{\epsilon_{\mathrm{max2}}} f(\epsilon)\mathrm{d}\epsilon + \int_{\epsilon_{\mathrm{max2}}}^{\epsilon_{\mathrm{max1}}} f(\epsilon)\mathrm{d}\epsilon\right) \tag{4.10}$$

where $\Delta L_{\nu_\alpha 1} = \Delta L_{\nu_\alpha}(\nu_\alpha \to \nu_{s1})$ and $\Delta L_{\nu_\alpha 2} = \Delta L_{\nu_\alpha}(\nu_\alpha \to \nu_{s2})$. What happens when the heavier state resonance is hit first and produces some amount of sterile neutrinos? How high is the abundance of the lower mass state relative to the heavier state? Is it possible to produce a sterile neutrino abundance that could account for DM with two or more resonances? Those are the questions that will be answered next.

Taking the heavier state as a point of reference

Since the resonance sweep is faster for the heavier state, it seems natural to decrease the lepton asymmetry by conversion to the heavier state first, $\Delta L_{\nu_\alpha 2} = \int_{\epsilon_{\mathrm{QCD2}}}^{\epsilon_{\mathrm{max2}}} f(\epsilon)\mathrm{d}\epsilon$, and then take a look at the lepton asymmetry depletion due to conversion to the lighter state: $\Delta L_{\nu_\alpha 1} = \int_{\epsilon_{\mathrm{max2}}}^{\epsilon_{\mathrm{max1}}} f(\epsilon)\mathrm{d}\epsilon$. The problem is that $\Delta L_{\nu_\alpha} = \Delta L_{\nu_\alpha 2} + \Delta L_{\nu_\alpha 1}$ is not known. What is known is $\Delta L_{\nu_\alpha \mathrm{eff}} = 2\Delta L_{\nu_\alpha 2} + \Delta L_{\nu_\alpha 1}$ due to the different masses entering the

abundance (see equation (4.10)):

$$\Delta L_{\nu_\alpha \mathrm{eff}} = \frac{\Omega^{SF}_{s1+s2} h^2}{0.0146\, m_{s1}/\mathrm{keV}} \tag{4.11}$$

$$= \int_{\epsilon_{\mathrm{max2}}}^{\epsilon_{\mathrm{max1}}} f(\epsilon)\mathrm{d}\epsilon + 2\int_{\epsilon_{\mathrm{QCD2}}}^{\epsilon_{\mathrm{max2}}} f(\epsilon)\mathrm{d}\epsilon. \tag{4.12}$$

Calculating a relative fraction of the first and second KK mode's abundance while requiring that the total abundance fulfills $\Omega^{SF}_{s1+s2}h^2 = \Omega_{DM}h^2 - \Omega^{DW}_{s1}h^2 - \Omega_{DM}h^2 - \Omega^{DW}_{s2}h^2$ does not yield any results. Leaving $\Delta L_{\nu_\alpha 1}$ as a free parameter, producing a fraction (say, 80 %, 10 %, or 1 %) of $\Omega^{SF}_{s1+s2}h^2$ via conversion into the second state and then looking at the yield from the subsequent conversion into the lighter state does not work either: the obtained result is an overclosure due to the later resonance staying adiabatic for too long.

Taking the lighter state as a point of reference

Now, one can assume that $\Delta L_{\nu_\alpha \mathrm{eff}} = \Delta L_{\nu_\alpha}$, solve the integral $\int_{\epsilon_{\mathrm{QCD2}}}^{\epsilon_{\mathrm{max1}}} f(\epsilon)\mathrm{d}\epsilon$ (assuming that the production relevant for today's abundance only starts at the higher ϵ_{QCD2} as we assume that the heavier state is produced reaonantly as well) and look for the cutoff ϵ_{max2}. This way, one overproduces sterile neutrino DM, but gets a measure of what fraction gets produced due to adiabatic conversion into the higher-mass state. The answer is: none. The lepton asymmetry required to not overproduce the lightest state is not sufficient to satisfy adiabaticity for the second lightest state.

The problem with adiabaticity

From section 3.2 we know that adiabaticity is crucial in an efficient conversion of active to sterile neutrinos. Let us therefore examine the adiabaticity condition (3.24) again:

$$4\cdot 10^8 \left(\frac{m_s}{\mathrm{keV}}\right)^{1/2} \left(\frac{\mathcal{L}}{10^{-3}}\right)^{3/4} \epsilon_{\mathrm{res}}^{-1/4} \sin^2 2\theta \left(1 - \frac{\mathrm{d}\mathcal{L}/\mathrm{d}t}{4H\mathcal{L}}\right)^{-1} \overset{!}{>} 1. \tag{4.13}$$

The term in brackets, $(1 - \frac{\mathrm{d}\mathcal{L}/\mathrm{d}t}{4H\mathcal{L}})^{-1}$ will always be ≥ 1 and $= 1$ when the (adiabatic) conversion stops. Since the lepton asymmetries and the spectral parameter are unknown, we can absorb everything else into a constant,

$$C := \left[4\cdot 10^8 \left(\frac{m_s}{\mathrm{keV}}\right)^{1/2} \sin^2 2\theta\right]^{-4/3} \tag{4.14}$$

and require that

$$C^{-1}\frac{\mathcal{L}}{10^{-3}}\,\epsilon_{\rm res}^{-1/3} \geq 1. \tag{4.15}$$

Since $m_{sk} \propto k$ and $\sin^2 2\theta_k \propto k^{-2}$, one can see that the constant C depends on the mode number k as well and $C_k \propto k^2$. The relation $\epsilon_{\rm QCD} \propto k^2$ is also known, so for the resonance to be adiabatic at a temperature of $T = 200$ MeV, the above condition translates to

$$\frac{\mathcal{L}}{10^{-3}} \geq C_k\,\epsilon_{{\rm QCD}k}^{1/3} \propto k^{8/3}. \tag{4.16}$$

Thus, the initial lepton asymmetry needs to be > 6.35 times higher for adiabatic conversion to take place to the second lightest state than it would be needed if only the first state is produced. Since the adiabaticity depends on the mixing angle $\sin^2 2\theta$, this implies that the condition might be fulfilled for larger mixing angles, requiring a smaller final lepton asymmetry. However, the resonance temperature equation is (3.14)

$$\frac{T_{\rm res}}{\rm MeV} \approx 90\left(\frac{m_s}{\rm keV}\right)^{1/2}\left(\frac{\mathcal{L}}{10^{-3}}\right)^{-1/4}\epsilon_{\rm res}^{-1/4} \tag{4.17}$$

and it is clear that during the conversion process the temperature has to go down (as the universe expands) as does the lepton asymmetry (as sterile neutrinos do not contribute to the lepton asymmetry). This means that the spectral parameter has to increase faster than the lepton asymmetry decreases. If this resonance condition is fulfilled for the second-lightest state, it will not be fulfilled for the lightest state (remember that the sweep rate across the resonance is slower for lighter modes). The high lepton asymmetry that is present will lead to an overabundance of the lightest sterile mode, overclosing the universe. On the other hand, if the resonance condition shall be fulfilled for both states, the adiabaticity condition (which requires a "slow" sweep across the resonance) will not be fulfilled for the heavier state. In short, there is no overlap of lepton asymmetry values that would generate some adiabatic conversion into the second mode while not overproducing the first mode.

4.1.3 The general picture: n modes

After finding that the first and second lightest sterile neutrino modes cannot both be produced adiabatically *and* together yield the correct abundance required to account for the DM, the next question to answer is how that situation changes when looking at n modes to be produced.

First, n modes, each with a non-resonant DW production mechanism, lower the abun-

dance that is needed to be generated resonantly. The DW production mechanism (3.3) only slightly depends on the mode number, $\Omega_k^{DW} h^2 \propto k^{-0.2}$, however, the equation is not valid for arbitrarily small mixing angles or arbitrarily large masses. For masses higher than 3.4 keV, the production happens before the QCD transition and the abundance is subsequently diluted. For very small mixing angles (smaller than $\mathcal{O}(10^{-11})$ or so), the high neutrino scattering rate will suppress oscillations. In short, we do not need to take an infinite amount of modes into account even in the DW scenario, as their contribution goes to zero with vanishing mixing angle. In the region of interest, not more than $10-15$ modes have a higher than negligible contribution to the DW abundance.
The difference between needed lepton asymmetries for subsequent modes decreases as you go up in the KK mode number and the lepton asymmetries start overlapping (see equation (4.16)). However, there is no known mechanism that enhances oscillations in the higher modes, say $n = 3, 4$ while suppressing it for the lower modes $n = 1, 2$. At the moment when adiabaticity is lost and effective production of a higher mode ceases, there is still lepton asymmetry left. And this lepton asymmetry will lead to the conversion of active neutrinos into lower modes, if such modes exist. Without inventing a mechanism that prefers to enhance oscillations into higher modes with lower mixing angles, a resonant production of more than one sterile neutrino state is not possible without overclosing the universe.

4.2 Two working examples

Now that we know how the masses and mixing angles affect the KK-tower contribution to the sterile neutrino abundance, let us look at some examples in the parameter space not excluded by observations. This implies masses $m_{s1} \gtrsim 3$ keV, and mixing angles $\sin^2 2\theta \lesssim 10^{-8}$ as shown in Figure 3.1. We will start with a lightest mode of 3 keV mass, for which the contribution of the non-resonant production needs to be taken into account. This is the lightest possible mass that is not excluded by current constraints, and thus offers a good starting point. Also, for a rather small mass of the sterile neutrino, the mixing angle can be somewhat higher, which makes the mode easier to observe. We will also investigate a 7.1 keV first mode which is an interpretation of the faint unidentified 3.55 keV photon line in the spectra of galaxy clusters and the Andromeda galaxy discovered earlier this year [4, 5].

$m_{s1} = 3$ keV, $\sin^2 2\theta_1 = 4 \cdot 10^{-10}$

Assuming a tower of sterile neutrinos with the first mode having a mass of $m_{s1} = 3$ keV and a mixing angle of $\sin^2 2\theta_1 = 4 \cdot 10^{-10}$ to an active neutrino with a mass of $m_a = 0.03$ eV (see Section 2.2), we can derive the following:
The non-resonant contribution to the sterile neutrino abundance is (3.3)

$$\Omega_{s1}^{DW} h^2 \approx 0.003 \tag{4.18}$$

produced at $T_{\rm Peak} \simeq 192$ MeV (3.5). It is obvious, that all higher modes are produced prior to the QCD phase transition, therefore their abundance will be diluted by a factor of roughly 10 (see section 3.1). Then we obtain $\Omega_{sk}^{DW} h^2 \approx 0.0028$ for the contribution from modes $k = 2 - 15$. Production of the $k = 10$ mode peaks at $T_{\rm Peak} \simeq 413$ MeV and for the $k = 15$ mode, $T_{\rm Peak} \simeq 473$ MeV. However, especially for the higher modes the temperatures of peak production lie so close together (about 12 MeV between subsequent peaks), that production is likely to overlap and the resulting contribution from each mode is even lower. The main result is that the higher modes give a combined contribution to the sterile neutrino abundance that is of the order of the non-resonant contribution of a mode produced before the QCD transition. We will approximate

$$\sum_{k(T_{\rm Peak})>200\,{\rm MeV}} \Omega_{sk}^{DW} h^2 \approx \Omega_{s1}^{DW} h^2 \tag{4.19}$$

where non-resonant production of the $s1$ state peaks after the QCD-transition. This should include contributions from all modes that can be accessed via oscillations and their damping due to both the active neutrino scattering rate and the overlap of production regions. Then, the total DW contribution is

$$\Omega_s^{DW} h^2 = \sum_{k(T_{\rm Peak})>200\,{\rm MeV}} \Omega_{sk}^{DW} h^2 + \Omega_{s1}^{DW} h^2 \approx 2\,\Omega_{s1}^{DW} h^2. \tag{4.20}$$

Then, the amount that needs to be produced via an adiabatic resonance for the sterile neutrino to account for DM is

$$\Omega_{s1}^{SF} h^2 = \Omega_{DM} h^2 - \Omega_s^{DW} h^2 \tag{4.21}$$

$$= 0.0146 \frac{\Delta L_{\nu_\alpha}}{10^{-3}} \frac{m_s}{\rm keV} \tag{4.22}$$

and we get $\Delta L_{\nu_\alpha} = \frac{0.114}{3 \cdot 0.0146} \cdot 10^{-3} = 2.6 \cdot 10^{-3}$. This abundance can be produced adiabatically for $\mathcal{L}^i = 8.5 \cdot 10^{-3}$ and $\mathcal{L}^f = 3.3 \cdot 10^{-3}$ as the initial and final effective

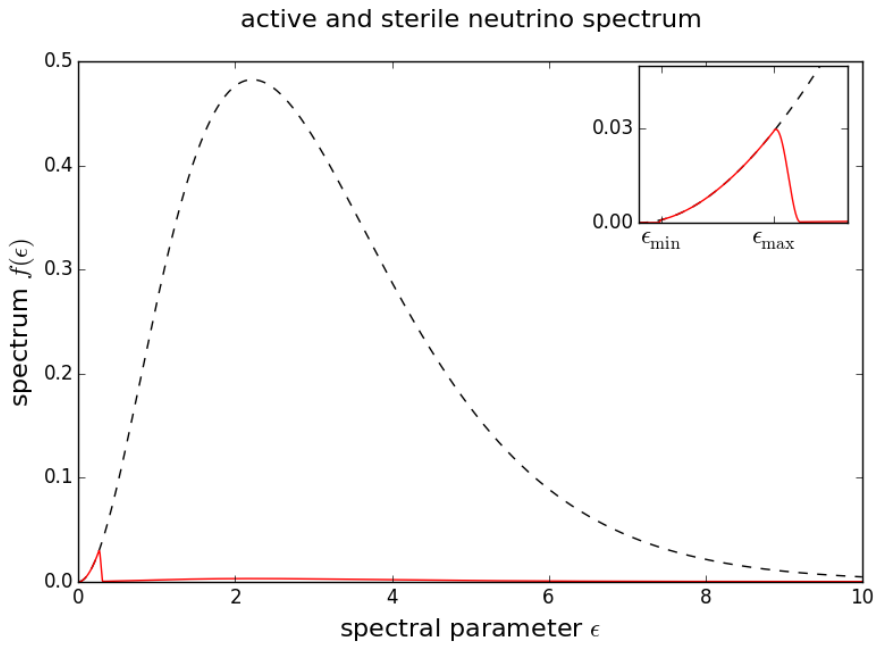

Figure 4.4: Thermal spectrum of the active neutrino (black) and part of the spectrum that is resonantly transformed into the lightest sterile mode with $m_{s1} = 3$ keV (red). The adiabatic transformation occurs for spectral parameters $0.043 < \epsilon < 0.259$ at the lower-energetic part of the spectrum leading to a colder-than thermal sterile neutrino spectrum.

lepton asymmetries respectively. The neutrinos that are transformed, have spectral parameters $0.043 < \epsilon < 0.259$, and are indeed at the lower end of the active neutrino spectrum as can be seen in Figure 4.4. The first sterile state with $m_{s1} = 3$ keV would have a photon with $E_\gamma = 1.5$ keV as decay signature .

$\mathbf{m_{s1} = 7.1\ keV,\ \sin^2 2\theta_1 = 7 \cdot 10^{-11}}$

If the mixing indeed follows the formula presented in (2.2), $\theta \approx \frac{m_a}{m_s}$, the sterile neutrino tower with a mass of the lightest KK state of $m_{s1} = 7.1$ keV and mixing angle $\sin^2 2\theta_1 = 7 \cdot 10^{-11}$ also implies an active neutrino with a mass of $m_a = 0.03$ eV. For this tower we obtain the following results:
The DW production peaks at a temperature of $T_{\text{Peak}} \simeq 256$ MeV, which is before the QCD transition. The $k = 8$ mode has a mixing angle of $\sin^2 2\theta_8 = 1.1 \cdot 10^{-12}$, so that the DW mechanism breaks down for higher modes, and peaks at $T_{\text{Peak}} \simeq 511$ MeV. We therefore take the first eight modes into account and dilute the obtained abundances as

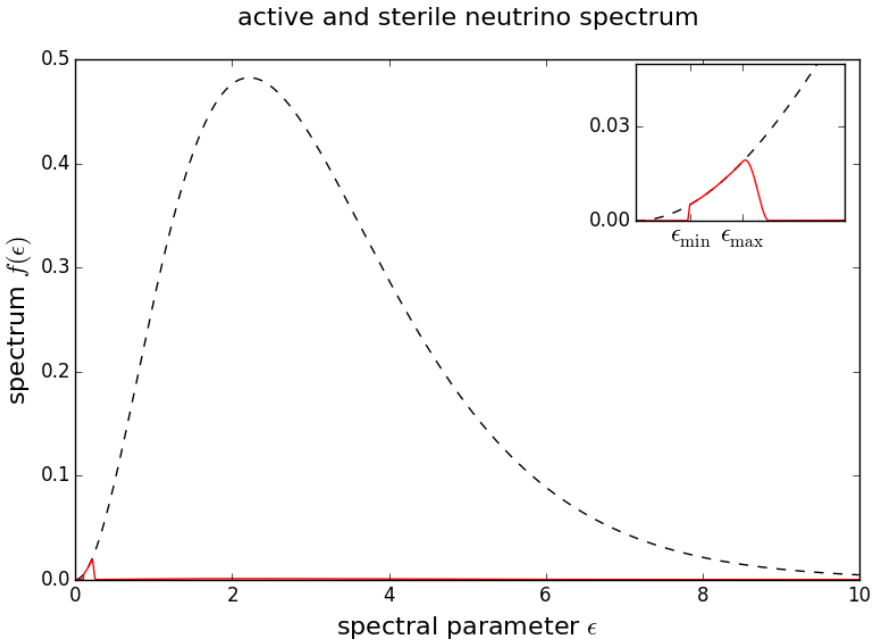

Figure 4.5: Thermal spectrum of the active neutrino (black) and part of the spectrum that is resonantly transformed into the lightest sterile mode with $m_{s1} = 7.1$ keV (red). The adiabatic transformation occurs for spectral parameters $0.104 < \epsilon < 0.205$ at the lower-energetic part of the spectrum.

before. The so-obtained non-resonant contribution to the sterile neutrino abundance is

$$\sum_{k=1}^{8} \Omega_{sk}^{DW} h^2 = 0.0015 \tag{4.23}$$

and the remainder of the DM abundance of $\Omega_{s1}^{SF} h^2 = 0.1184$ has to come from resonant production of the first mode. To obtain this abundance, a change in the lepton asymmetry in the oscillating flavor of $\Delta\mathcal{L} = 1.14 \cdot 10^{-3}$ is needed. This abundance can be produced adiabatically for $\mathcal{L}^i = 19.9 \cdot 10^{-3}$ and $\mathcal{L}^f = 17.6 \cdot 10^{-3}$ as the initial and final effective lepton asymmetries respectively. The neutrinos that are transformed have spectral parameters $0.104 < \epsilon < 0.205$, and also for this case are at the lower end of the active neutrino spectrum as can be seen in Figure 4.5. The required lepton asymmetry to generate a large enough sterile neutrino abundance to make up the DM is for this state quite high, but does not violate present-day constraints.

4.3 The influence of the full KK-tower on the sterile neutrino DM abundance

Summing up the findings of this chapter, we can answer the question how the sterile neutrino abundance is influenced by the extra-dimensional setting. The final picture we get for the KK-tower of sterile neutrinos with resonant and non-resonant production making up (most of) the DM is the following:

- The lightest state is produced resonantly in the Early Universe via the SF mechanism. It needs a non-zero lepton asymmetry to be present. Depending on its mass and mixing to the active neutrino, a large fraction of the initial lepton asymmetry may be left after resonant production ceases.
- Multiple states (including the lightest one) are produced non-resonantly via oscillations, as described by the DW mechanism. The number of states that is accessible via oscillations depends on the mixing of the states to the active neutrino.
- For the mixing of interest, $\sin^2 2\theta \approx \mathcal{O}(10^{-9} - 10^{-11})$, the DW abundance is much smaller than the overall DM abundance. Therefore, if KK states of sterile neutrinos make up the DM, most of the abundance comes from the resonant production of the lightest KK state.
- States more massive then ~ 3.4 keV are produced non-resonantly before the QCD phase transition. The phase transition leads to a decrease of the number of effective degrees of freedom and therefore to a dilution of the non-resonantly produced abundance.
- For very small mixing angles $< \mathcal{O}(10^{-11})$ or so, the DW mechanism breaks down as the neutrino interaction rate inhibits the oscillation.

We can conclude that the tower of sterile neutrinos does not play any significant role in the generation of the sterile neutrino abundance, and only has a negligible influence on the DM abundance today, if sterile neutrinos are the DM.

4.4 Sterile neutrinos as Warm Dark Matter

According to its properties, DM can be split up into three categories: Hot, Warm, and Cold. Which category a DM candidate falls into, depends on its properties when it comes to forming structures. This is often described by the species' free-streaming

length. However, the question when a DM particle is "warm" and when it is "cold" is not that easy to answer. Historically, only two categories existed, HDM and CDM. In the standard picture, both are produced in the Early Universe via interactions with SM particles that are of order of the strength of the weak force, but their interactions freeze out at some point. This moment of freeze-out occurs when the particle's interaction rate falls below the expansion rate of the universe, such that the particle drops out of equilibrium. Besides sharing the standard production schemes and both being collisionless, HDM and CDM have opposite properties. HDM is relativitic up to very late times, therefore it has a very large free-streaming length and suppresses early structure formation. A HDM universe would look very different from the one we are living in as it would have formed in a top-down scenario, with superclusters forming first and later fragmenting into clusters and galaxies. Observations of the universe's structures proved to be in conflict with HDM predictions, thus this category of DM was ruled out rather long ago [39]. However, HDM had a clear advantage: there is a SM particle that is HDM - the neutrino. It is light and remains relativistic until late times. However, from the combination of multiple observations we know that the standard active neutrinos have a sum of masses of $\sum m_\nu < 0.23$ eV [12] and thus HDM can make up less than 1.5 % of the matter density of the universe.

The other category postulated early on is CDM. It is non-relativistic at the time its intereactions decouple and the species freezes out. After freeze-out, it clumps readily forming gravitational wells. Ordinary matter falls into these wells forming overdense regions and finally visible structures. As time goes by, proto-galaxies evolve and merge into larger galaxies and clusters to finally form the largest structures of the universe [39]. A favourite CDM candidate is the WIMP, the Weakly Interacting Massive Particle. Its high mass ensures that it clumps early-on, while its weak interactions make it possible to detect WIMPS. To-date, no WIMPS were observed (the few claims of discoveries that were made were either refuted by the collaborations themselves or lie in regions excluded by other experiments). A possible way out is to postulate weaker-than-weak, or, feeble, interactions between SM and CDM particles, and call those particles FIMPS – Feebly Interacting Massive Particles. Obviously, they would be more difficult to find with present-day experiments, thus explaining the lack of discoveries.

However, CDM has another problem apart from not being discovered yet. It likes to clump too much. As it has a negligible free-streaming length, it would form all kinds of structures on all scales. But this is not what we observe. We observe far fewer dwarf galaxies than we would expect from CDM simulations. On the other hand, dwarf galaxies are too big to evade discovery at least in our galactic neighborhood. With no known

mechanism that suppresses the formation of dwarf galaxies and accounts for the observed cutoff scale, this problem has become known as the "missing satellite" problem. It is closely linked to the "too big to fail" problem, which states that based on simulations there are many predicted Milky Way subhalos too massive to not host stars (i.e. more massive than known dwarf galaxies).
There are multiple ideas of how to solve the problems with CDM. One is to look at a mixture of HDM and CDM where the hot component would be just enough to dilute the small scale structures, but small enough to not hinder early LSS formation. Another idea is that of baryonic matter feed-back. The baryonic matter could come from supernovae and lower the subhalo core densities by gas removal to match the observations. However, this mechanism alone cannot solve the problem [45].
A different approach is to change the properties of the DM particles themselves. Instead of being cold and having low velocities already in the very Early Universe, it is possible that they are somewhat inbetween cold and hot. Therefore, this DM type is referred to as "warm". WDM is relativistic in the very Early Universe, but becomes non-relativistic early enough to allow for a CDM-like LSS formation. However, WDM has a non-negligible free-streaming length, usually set to scales of dwarf galaxies. This implies, that only structures bigger than the free-streaming length can form.
The "warmth" of the DM particle is oftentimes related to its mass, but the really relevant properties are the dynamical ones such as the average momentum, or free-streaming length at matter-radiation equality. The particle's mass is only a good indicator of "warmth" if the production mechanism is that of the thermally produced particle whose interactions freeze-out at some point.

4.4.1 Properties of resonantly produced keV sterile neutrino DM

A good reference of the "warmth" of a particle species is its characteristic free-streaming length. The free-streaming length defines the scale below which density fluctuations are damped. For active neutrinos, this length was derived as [46]:

$$\lambda_{fs} \sim 40 \left(\frac{30\text{eV}}{m_\alpha} \right) \text{Mpc}. \tag{4.24}$$

As a thermal sterile neutrino produced via the DW mechanism has the same thermal spectrum as the initial active neutrino species ν_α, (4.24) applies with $m_\alpha \to m_s$. The sterile neutrino produced resonantly has a colder spectrum, and a larger free-streaming

lenght than a thermal sterile neutrino of the same mass [32]

$$\lambda_{fs} \sim 40 \left(\frac{30\text{eV}}{m_s}\right) \left(\frac{\langle\epsilon\rangle}{3.15}\right) \text{Mpc} \tag{4.25}$$

where $\langle\epsilon\rangle$ is the average sterile neutrino spectral parameter and 3.15 is the average spectral parameter for active and thermally produced sterile neutrinos. For the sterile neutrinos produced with the SF mechanism in the previous chapter, the average spectral parameter can be approximated by $\int_0^{\langle\epsilon\rangle} \frac{\epsilon^3 \mathrm{d}\epsilon}{e^{\epsilon-\xi}+1} \approx 8/3\Delta L_{\nu_\alpha}$ [32] which for $m_{s1} = 7.1$ keV (3 keV) results in $\langle\epsilon\rangle \approx 0.4$ (0.5). We then obtain $\frac{\langle\epsilon\rangle}{3.15} \sim 0.13$ (0.16), leading to free-streaming lengths of 0.02 Mpc (0.06 Mpc). This is very roughly the radius of the Milky Way's disc. Using (4.24), the resonantly produced sterile neutrinos correspond to thermal sterile neutrinos with masses of 55 keV (for the 7.1 keV produced sterile neutrino) and 19 keV (for the 3 keV resonantly produced neutrino), well outside of current bounds.

Chapter 5

Experimental signature 1: radiative decay

In order to be a viable DM candidate, a particle must have a much longer lifetime than the age of the universe. The prospects for long sterile neutrino lifetimes are good: without additional interactions, the decay of sterile neutrino states will be suppressed by the active-sterile mixing angle. On the other hand, this tiny mixing angle allows not only for the production of sterile neutrinos but also for their decay. In this chapter, we will study the properties of sterile neutrinos that are important today: their lifetimes and decay signatures.

5.1 Decay modes

As the sterile neutrino has a very small mixing with the active neutrino, it can decay. The main decay mode, depicted in Figure 5.1, is invisible, as the final state consists of

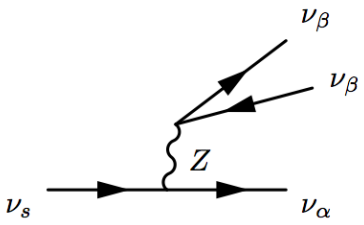

Figure 5.1: Tree-level diagram for the decay process $\nu_s \to \nu_\alpha \nu_\beta \overline{\nu}_\beta$ where ν_β can be any active neutrino flavor.

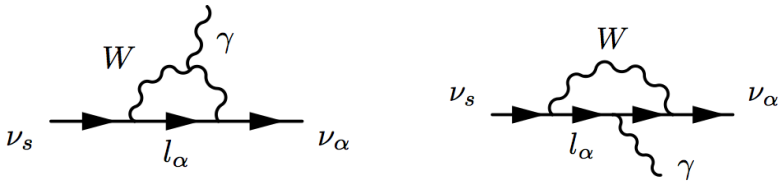

Figure 5.2: One-loop diagrams for the decay process $\nu_s \to \nu_\alpha \gamma$.

three active neutrinos [33, 35]:

$$\Gamma_{\nu_s \to 3\nu} = \frac{G_F^2 m_s^5}{192\pi^3}\theta^2 \tag{5.1}$$

$$\approx 8.7 \cdot 10^{-31} s^{-1} \left(\frac{\sin^2 2\theta}{10^{-10}}\right) \left(\frac{m_s}{\text{keV}}\right)^5 \tag{5.2}$$

where $3\nu = \nu_\alpha \nu_\beta \overline{\nu}_\beta$. This decay mode dominates the sterile neutrino's lifetime. The strongest visible decay mode is the one loop suppressed decay $\nu_s \to \nu_\alpha \gamma$ shown in Figure 5.2. As the active ν_α is highly relativistic, both decay products – the active neutrino and the photon – have an energy of $E_{\nu_\alpha} = E_\gamma = m_s/2$. This narrow line can be searched for with telescopes. This decay is suppressed by a factor of $\frac{27\alpha_{FS}}{8\pi}$ relative to the 3ν decay [47]:

$$\Gamma_{\nu_s \to \nu_\alpha \gamma} = \frac{27\alpha_{FS}}{8\pi} \frac{G_F^2}{192\pi^3} \left(\frac{m_s^2 - m_a^2}{m_s}\right)^3 \left(m_s^2 + m_a^2\right) \theta^2 \tag{5.3}$$

where α_{FS} is the fine structure constant. For $m_a \ll m_s$ this can be rewritten as [33]

$$\Gamma_{\nu_s \to \nu_\alpha \gamma} = \frac{9\alpha_{FS} G_F^2}{2048\pi^4} m_s^5 \sin^2 2\theta \tag{5.4}$$

$$\approx 6.8 \cdot 10^{-33} s^{-1} \left(\frac{\sin^2 2\theta}{10^{-10}}\right) \left(\frac{m_s}{\text{keV}}\right)^5 . \tag{5.5}$$

The lifetime is just the inverse of the sum of the decay rates of all possible decay modes i, and is given as

$$\tau = \left(\sum_i \Gamma_i\right)^{-1} . \tag{5.6}$$

Since the radiative decay (5.5) accounts for less than one percent of the decays, we will just approximate $\tau = \Gamma^{-1}_{\nu_s \to \nu_\alpha \gamma}$ to simplify calculations. We can then write

$$\tau \approx \frac{192\pi^3}{G_F^2} m_s^{-5} \theta_s^{-2} \tag{5.7}$$

$$\approx 1.1 \cdot 10^{30} s \left(\frac{\sin^2 2\theta}{10^{-10}} \right)^{-1} \left(\frac{m_s}{\text{keV}} \right)^{-5}. \tag{5.8}$$

One can now easily see that for all possible values of sterile neutrino masses and mixing angles in agreement with WDM bounds the condition of the lifetime being much larger than the age of the universe of $\tau_U \sim 4.3 \cdot 10^{17} s$ [12] is satisfied.

5.2 Stability of the states

We will now calculate how the stability of the states depends on their mode number, and apply the results to our two working examples from section 4.2 and calculate their lifetimes. It is clear that the states need to have a much longer lifetime than the age of the universe to be viable DM candidates.

5.2.1 Decay modes and stability of higher states

From (5.2) and (5.5) we see that $\Gamma \propto m_{sk}^5 \sin^2 2\theta_k^2$ for both decay modes ($\nu_{sk} \to 3\nu$ and $\nu_{sk} \to \nu_\alpha \gamma$), therefore for the k-th KK mode

$$\Gamma_{\nu_{sk}} \propto k^5 m_{s1}^5 k^{-2} \sin^2 2\theta_1 \tag{5.9}$$

$$\propto k^3 m_{s1}^5 \sin^2 2\theta_1, \tag{5.10}$$

thus the lifetime is $\tau_{sk} \propto k^{-3}$. We see that the higher states have sharply decreasing lifetimes.

The excited states can also decay into the lowest state, this decay mode is shown in Figure 5.3. But this decay is doubly suppressed by the mixing angle in our model without additional mixing within the KK tower. As the W bosons only interact with active neutrinos, both interactions ($\nu_{sk} \to W + l_\alpha$ and $W + l_\alpha \to \nu_{s1}$) are suppressed by the active-sterile mixing angle ($\sin^2 2\theta_k$ and $\sin^2 2\theta_1$ respectively). Evaluating (5.3) we

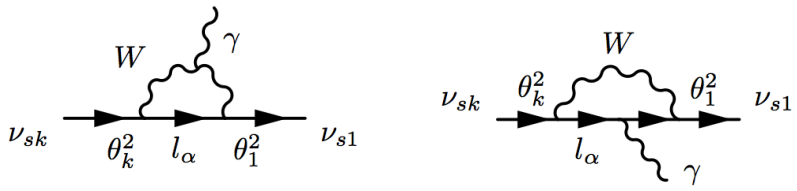

Figure 5.3: One-loop diagrams for the decay process $\nu_{sk} \to \nu_{s1}\gamma$, which is doubly suppressed by the active-sterile mixing angles.

arrive at

$$\Gamma_{\nu_{sk}\to\nu_{s1}\gamma} = \frac{9\alpha_{FS}G_F^2}{2048\pi^4}\left(\frac{m_{sk}^2 - m_{s1}^2}{m_{sk}}\right)^3 \left(m_{sk}^2 + m_{s1}^2\right)\sin^2 2\theta_k \sin^2 2\theta_1 \tag{5.11}$$

$$= \frac{9\alpha_{FS}G_F^2}{2048\pi^4}\frac{(k^2-1)^3(k^2+1)}{k^5} m_{s1}^5 \sin^4 2\theta_1 \tag{5.12}$$

$$\propto (k^3 - 2k + 2/k^3 - 1/k^5)\sin^2 2\theta_1\, \Gamma_{\nu_{s1}\to\nu_\alpha\gamma}. \tag{5.13}$$

As $\sin^2 2\theta_1 \approx \mathcal{O}(10^{-10} - 10^{-12})$, for all $k \sim \mathcal{O}(10)$ modes of interest, the decay into the lightest sterile neutrino mode is highly suppressed. The decay to intermediate modes ($\nu_{sk} \to \nu_{sj}\gamma$, $k > j$) leads to a more complicated expression for the decay rate, but to the same qualitative result. Without an additional mixing within the sterile neutrino tower, decay of higher sterile neutrino modes to lower ones is highly suppressed.

5.2.2 Examples of sterile neutrinos with long lifetimes

We will now turn to our two examples from section 4.2, with $m_{s1} = 3$ keV, $\sin^2 2\theta_1 = 4 \cdot 10^{-10}$ and $m_{s1} = 7.1$ keV, $\sin^2 2\theta_1 = 7 \cdot 10^{-11}$ and calculate their expected lifetimes.

The $\mathbf{m_{s1} = 3}$ keV, $\mathbf{\sin^2 2\theta_1 = 4 \cdot 10^{-10}}$ case

The sterile neutrino with a mass of $m_{s1} = 3$ keV can decay via the process shown in Figure 5.2 emitting a photon of energy $E_\gamma = 1.5$ keV, or half the sterile neutrino's mass. Plugging in the parameters into (5.2) we get for the lifetime of the $k = 1$ mode:

$$\tau_{s1} \approx \Gamma^{-1}_{\nu_s\to 3\nu} \approx 1.2 \cdot 10^{27}\, s. \tag{5.14}$$

This is much longer than the age of the universe of $\tau_U \sim 4.3 \cdot 10^{17}\, s$. The long lifetime indeed makes this sterile neutrino a good WDM candidate. For the second lightest state, we obtain $\tau_{s2} \approx 1.5 \cdot 10^{26}\, s$ and for the third state, $\tau_{s3} \approx 4.4 \cdot 10^{25}\, s$. The lifetime of

the kth state is $\propto k^{-3}$, but as the first state has a lifetime exceeding the age of the universe by ~ 10 orders of magnitude, the higher modes are also stable. If they had been produced in a bigger amount in the Early Universe, they could also contribute to the DM density today.

The $\mathbf{m_{s1} = 7.1}$ keV, $\mathbf{\sin^2 2\theta_1 = 7 \cdot 10^{-11}}$ case

With the same approach as above, we get

$$\tau_{s1} \approx 9.1 \cdot 10^{25}\, s \tag{5.15}$$

for the lifetime of the $k = 1$ mode, which again exceeds the age of the universe by a few orders of magnitude. For the second lightest state, we obtain $\tau_{s2} \approx 1.1 \cdot 10^{25}\, s$ and for the third state, $\tau_{s3} \approx 3.4 \cdot 10^{24}\, s$. As for the previous example, the excited states are stable (on the timescale of the age of the universe) as well. In a scenario where this $m_{s1} = 7.1$ keV, $\sin^2 2\theta_1 = 7 \cdot 10^{-11}$ sterile neutrino is the DM and comes with an insignificant abundance of higher modes, the modes do not completely decay in the Early Universe but would still be around today.
The long lifetime of the lightest mode makes it a good WDM candidate. It also supports the suggestion that this sterile neutrino might account for the recently found weak 3.55 keV line as a decaying DM particle.
For both examples of a sterile neutrino tower given here, there is no early decay of heavy modes with entropy injection as is usually assumed for models with one keV sterile neutrino and further heavy sterile neutrinos (see e.g. [35]). However, those heavy sterile neutrinos usually have masses many orders of magnitude larger than the higher KK states in our model.

5.3 Observation of radiatively decaying sterile neutrinos

The best chance to find a sterile neutrino from astrophysical observations presents itself in the search for previously unidentified narrow spectral lines, with $E_\gamma = m_{s1}/2$. Those searches can be also used to constrain a large fraction of the sterile neutrino parameter space, and were used to produce Figure 3.1 [5].
Recently, two independent groups announced an observation of a spectral line at 3.55 keV, that could not be accounted for by any known atomic or molecular transitions. The authors of [5] used the satellite XMM-Newton and observed a stack of 73 galaxy clusters in the redshift range of $0.01 \leq z \leq 0.35$. They removed known lines (e.g. due

to atomic transitions) from the clusters' spectra, stacked the spectra and corrected for redshift. With this method all instrumental features should be greatly suppressed (as they would appear at fixed energies in the spectra and be washed out by the redshift correction), while very weak lines in the spectra themselves would be enhanced (as they should be present at the same redshift-corrected position in all samples). This allowed the group to see features in the full stack and also in subsamples that might have remained hidden if each cluster's spectrum was evaluated individually. They found a line at $E_\gamma = (3.55 - 3.57) \pm 0.03$ keV using two different instruments onboard of the XMM satellite. They also find the same line in the spectrum of the Perseus cluster using data from the Chandra satellite, but do not observe the line in all individual subsamples. They argue that a good explanation for this line is given by a decaying sterile neutrino with a mass of 7.1 keV and a mixing of $\sin^2 2\theta \approx 7 \cdot 10^{-11}$. However, they also stress that the line is very weak and at the limit of the current instruments. Also, known atomic transition lines in the vicinity of the 3.55 keV line add to the uncertainty in the modelling of the spectra. Another problem is with the explanation of the line's origin: in comparison with other clusters, the line seems to be too bright in the Perseus cluster spectrum for the cluster's mass and distance.

The authors of [4] also use the XMM-Newton observatory and see a line of $E_\gamma \sim 3.5$ keV in the spectra of the Perseus cluster and the Andromeda galaxy. They do not stack spectra of multiple objects to remove instrumental lines, but focus on objects for which there exists good observational data. They not only find the line, but also observe how it gets stronger toward the centers of the observed objects – in agreement with expectations from a decaying DM particle hypothesis. Further, in a blank-sky data set, the line was absent, which speaks against it being an instrumental feature.

Since these observational claims were first published in February 2014, there have been numerous publications on that topic. The authors of [4] observed the line at $E_\gamma = 3.539 \pm 0.011$ keV in the Milky Way center [48]. However, several other groups could not observe the line in dwarf spheroidal galaxy [49] or stacked galaxy [50] spectra, or they observed a very faint line in galactic spectra but interperpreted it as being due to enhanced atomic transitions [51, 52]. The status of the line is inconclusive (see also a summary of present findings in [53]) and its interpretation hotly debated. However, the authors of [54] show that a deep observation of the Draco dwarf spheroidal galaxy with the present-day XMM-Newton satellite would prove or rule out the existence of the 3.55 keV line at a statistical significance of 3σ while the authors of [55] conclude, after studying the line's morphology in detail for the Galactic Center and the Perseus cluster, that the line exists but a DM origin is unlikely and instead an astrophysical origin is

favored.
Likewise, there have been numerous publications on the nature of the decaying DM particle that would also be consistent with the 3.55 keV line. Some authors followed the hypothesis presented by the original authors of the 3.55 keV line. They investigated sterile neutrinos arising from different models being the decaying DM particle responsible for the line (see e.g. [56]). But also other candidates have been proposed as explanation of the 3.55 keV line, including axions [57], scalar DM [58], supersymetric particles [59] or dark atoms [60] to name a few.

5.4 Observability of a sterile neutrino tower

As follows from our previous calculations presented in chapter 4 and section 5.2, the decay that is most likely to be observed is the $\nu_{s1} \to \nu_\alpha \gamma$ decay. This is due to two reasons: first, the first state $s1$ gets produced with by far the highest abundance (the remaining higher states are just corrections at the $\sim 1\,\%$ level) and second, the radiative decay of the higher states is not enhanced enough to make up for the deficit of the higher states' abundance.
The higher modes of a sterile neutrino tower have a negligible influence on the DM abundance, and therefore their decay would only produce a negligible flux. In short, within the model considered here, higher modes are not likely to be observed with any present or next-generation astrophysical instruments. There is no observable influence of the KK-tower on the DM abundance or spectral features.
The non-observability of the higher modes in astrophysical line searches is a good justification for only considering the 3.55 keV line as the result of a decaying lightest mode sterile neutrino in chapter 4. We have not considered the possibility of the 7.1 keV sterile neutrino being the second lightest state, as it would not have been produced in an amount that would make it observable. On the other hand, if spectral lines from the decay of higher modes were observed, this would imply that there is another generation mechanism, leading to an enhanced production of the higher states in the Early Universe and their larger abundance today. To observe the influence of the higher modes, astrophysical line searches are not well-suited. We will discuss searches in β-decays and whether they are more likely to observe higher modes in the next chapter.

Chapter 6

Experimental signature 2: β-decay

Sterile neutrinos are not only produced via oscillations in the Early Universe. Of course any active neutrino that has a high enough energy can oscillate into a sterile state, given a non-zero active-sterile mixing angle. The probability of oscillations is tiny (the oscillation depth is $\sin^2 2\theta_k$), but still can lead to interesting signatures, e.g. in nuclear β-decay.

6.1 The β-decay as a probe of neutrino mass

While cosmological measurements of the neutrino mass have a higher sensitivity, they are highly model-dependent. Measurements of the β-decay spectrum on the other hand are model-independent. Unlike neutrinoless double beta decay (which is possible only if neutrinos are Majorana particles), single beta decay does not depend on the nature of the neutrino (Dirac or Majorana). In β-decay, a neutron inside a nucleus transforms weakly into a proton, an electron and an electron antineutrino:

$$(A, Z) \rightarrow (A, Z + 1) + e + \overline{\nu}_e \tag{6.1}$$

where A is the mass number and Z the atomic number of the nucleus. Alternatively, the above equation can be written as

$$n \rightarrow p + e + \overline{\nu}_e. \tag{6.2}$$

If this process didn't involve neutrinos, it would be a two-body decay, with the electron having a fixed energy – the β-spectrum would be a mono-energetic line. However, instead a continuus spectrum is observed. It was this observation that initially led Pauli

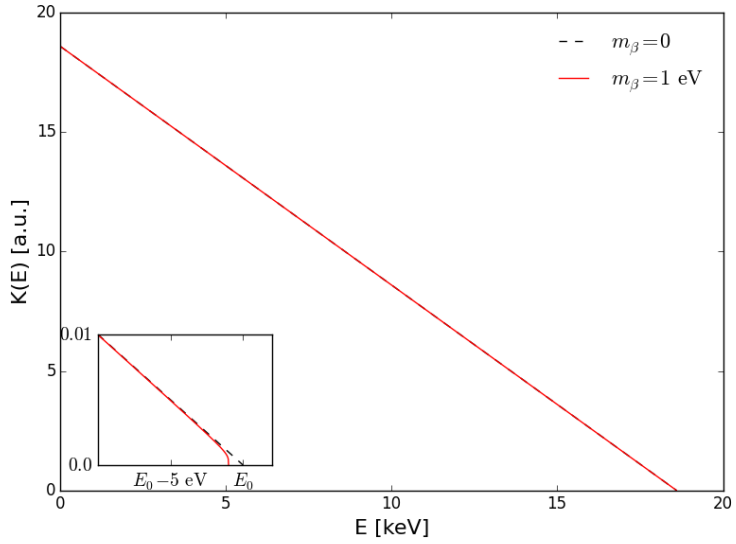

Figure 6.1: Kurie function of Tritium β electrons for zero neutrino mass (dashed black) and for $m_\beta = 1$ eV (solid red). The endpoint energy is $E_0 = 18.6$ keV.

to postulate a new particle in 1930 which later became known as the neutrino.
The β-spectrum is very sensitive to the effective mass of the electron anti-neutrino $m_{\overline{\nu}_e,\text{eff}} \equiv \langle m_\beta \rangle$. Note that the index β in m_β now refers to the β-decay production process, not a neutrino flavor. A non-zero effective neutrino mass changes the β-spectrum, the largest deviation from a spectrum with zero effective neutrino mass is near the endpoint energy. At the endpoint energy, the electron carries away all of the available kinetic energy from the decay process, the neutrino being released at rest. The influence of a non-zero effective neutrino mass is shown in Figure 6.1. Since the neutrino is produced in the electron flavor eigenstate, which is a superposition of all mass eigenstates weighted by their relative admixture to the flavor eigenstate, the beta decay spectrum is sensitive to the effective mass of an electron anti-neutrino

$$\langle m_\beta \rangle^2 = \sum_i |U_{ei}|^2 m_i^2. \tag{6.3}$$

The energy distribution of tritium beta decay electrons as measured by a β-decay experiment is [61]

$$\frac{\mathrm{d}\Gamma}{\mathrm{d}E} = F(E,Z) \cdot (E_0 - E)\sqrt{(E_0 - E)^2 - m_\beta^2}\ \Theta(E_0 - E - m_\beta), \tag{6.4}$$

where E is the electron energy, E_0 is the endpoint energy and Θ is the Heaviside function. $F(E,Z)$ is given by

$$F(E,Z) = G_F^2 \frac{m_e^5}{2\pi^3} \cos^2\theta_c |M|^2 R(E,Z) pE \tag{6.5}$$

where θ_c is the Cabbibo angle, $|M|$ is the nuclear matrix element and $R(E,Z)$ accounts for the Coulomb interaction between the electron and the daughter nucleus. The Kurie function is defined as

$$K(E) = \sqrt{\frac{\mathrm{d}\Gamma/\mathrm{d}E}{F(E,Z)}}. \tag{6.6}$$

For $m_\beta = 0$, the Kurie function is a straight line. Any deviation from a straight line is then due to a nonzero m_β. This fact is used in direct measurements of the neutrino mass using β-decay.

6.1.1 β-decay experiments: results and future

At present, the most sensitive laboratory experiments directly measuring the effective electron neutrino mass are β-decay experiments. Tritium is a β-electron emitter that is very well suitable for neutrino mass searches. It was used in the Mainz and Troitsk experiments, and will be used in the upcoming KATRIN experiment. The β decay of Tritium to Helium is

$$^3_1H \rightarrow ^3_2 He + e + \overline{\nu}_e \tag{6.7}$$

with an endpoint energy of $E_0 = 18.6$ keV and a half-life of $\tau_{1/2} = 12.3$ years [61]. The decay time offers a good combination of a high count rate and a good stability over the measurement time.

The most stringent upper bounds from direct measurements of the neutrino mass come from the Mainz (taking data from 1997 to 2001) and Troitsk (taking data from 1994 to 2004) experiments. The experiments place an upper bound on the effective electron anti-neutrino mass of $m_{\overline{\nu}_e,\mathrm{eff}} \equiv \langle m_\beta \rangle < 2$ eV [2].

As the highest deviation from a spectrum without neutrino mass is close to the endpoint energy, the Mainz and Troitsk experiments concentrated data taking on the highest-energy part of the spectrum. To cut away the low-energy part of the spectrum, a retarding (or filter) potential was applied, so that only the electrons with a higher energy could pass on to the detector. However, only a fraction of $\sim 2 \cdot 10^{-13}$ of all emitted electrons fall in the last 1 eV of the spectrum. This requires a long time of data taking. The upcoming KATRIN (KArlsruhe TRitium Neutrino) experiment [61] aims at

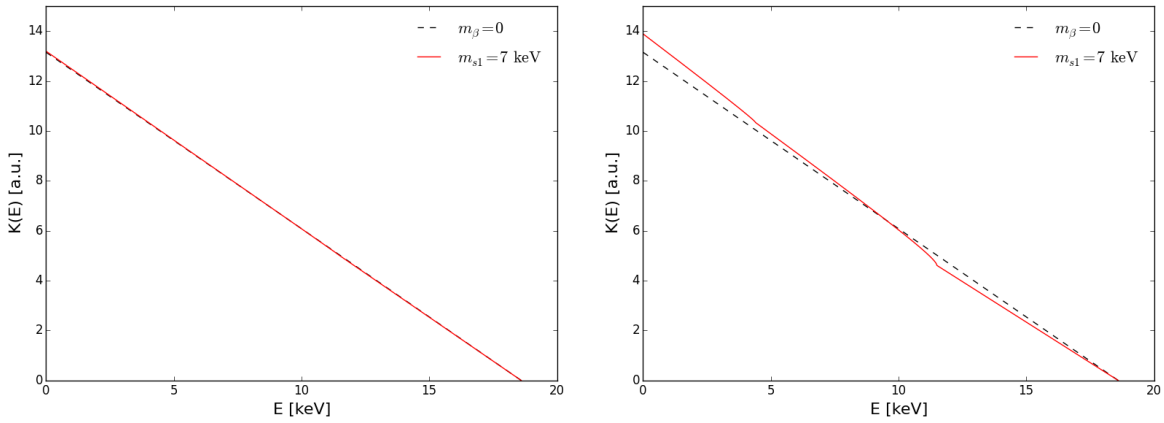

Figure 6.2: Kurie functions of Tritium beta decay electrons. **Left:** Kurie function for zero neutrino mass (dashed black) and with a tower of sterile neutrinos with $m_{s1} = 7.1$ keV and $\sin^2 2\theta_1 = 7 \cdot 10^{-11}$ (solid red). In principle, the first two states are accessible. **Right:** The tower has $m_{s1} = 7.1$ keV and $\sin^2 2\theta_1 = 0.5$ (solid red). Now two kinks from the first two states are visible.

improving the current bounds by an order of magnitude. Data taking is supposed to start in 2016 [62] and take three years. While KATRIN will measure electrons close to the endpoint of the spectrum to increase sensitivity to the neutrino mass, upgrades are possible which may be sensitive to sterile neutrinos [63]. For a sterile neutrino search, the whole spectrum would have to be scanned, looking for kink-like features in the count rate. This however requires an upgrade of the detector system for the high count rates far away from the endpoint.

6.2 Influence of a sterile neutrino tower on the β-decay spectrum

If the electron neutrino mixes with sterile neutrinos ($\alpha = e$ in the previous chapters), the presence of the sterile neutrino tower affects the β-spectrum. With one sterile neutrino present, the effective mass of the electron neutrino can be written as

$$\langle m_\beta \rangle^2 = \sum_{i=1}^{4} |U_{ei}|^2 m_i^2 \tag{6.8}$$

$$= \cos^2\theta \, m_{\text{light}}^2 + \sin^2\theta \, m_s^2 \tag{6.9}$$

where the effective light mass, $m_{\text{light}} = \sum_{i=1}^{3} |U_{ei}|^2 m_i^2$ and the heavy sterile neutrino mass is m_s with θ being the active-sterile mixing angle. The energy distribution of the beta decay electrons is then changed to [63]

$$\frac{\mathrm{d}\Gamma}{\mathrm{d}E} = \cos^2\theta \frac{\mathrm{d}\Gamma}{\mathrm{d}E}(m_{\text{eff}}) + \sin^2\theta \frac{\mathrm{d}\Gamma}{\mathrm{d}E}(m_s) \tag{6.10}$$

where $\frac{\mathrm{d}\Gamma}{\mathrm{d}E}(m_{\text{eff}})$ is given by (6.4). The light neutrino mass m_{light} is so small that it cannot be resolved with any near-future experiment, therefore it appears as one effective term. In general, the sterile neutrino is not restricted to mix with the electron neutrino. However, the β-decay investigates electron neutrinos, therefore the electron-flavor neutrino has to mix with the sterile neutrinos for them to leave an imprint on the β-spectrum. The description of the influence of one sterile neutrino can easily be extended to a tower, where all sterile modes with $m_s < E_0$ have to be taken into account. All those modes then have to be included in (6.4) and (6.9). The influence of a sterile neutrino tower with $m_{s1} = 7.1$ keV on the Kurie function is shown in Figure 6.2. On the left, the function is shown for the example investigated before, that coincides with the recently found 3.55 keV line, with a mixing angle of $\sin^2 2\theta_1 = 7 \cdot 10^{-11}$. On the right, the same mass sterile neutrinos have a mixing angle of $\sin^2 2\theta_1 = 0.5$. Such a large mixing is of course ruled out, but is shown here as a visualisation of how the sterile states qualitatively influence the β spectrum. Two states can be accessed in Tritium β-decay, if $m_{s1} = 7.1$ keV.

6.2.1 Number of observable states

Figure 6.3 shows two examples of the difference between the Kurie functions without and with sterile states present. The examples used coincide with our previously investigated towers. On the left side of Figure 6.3, the influence of the tower with $m_{s1} = 3$ keV and $\sin^2 2\theta_1 = 4 \cdot 10^{-10}$ is shown. While the five lightest states are in principle accessible, only the lightest three states produce a kink that is visible on the logarithmic scale. On the right side, the second tower investigated, with $m_{s1} = 3$ keV and $\sin^2 2\theta_1 = 4 \cdot 10^{-10}$ is shown. Both states accessible are visible on the logarithmic scale. The crossing, visible in both plots as the region where the difference goes to zero, is due to normalisation: In the presence of sterile states, the count rate will be slightly lower at low energies and slightly higher at high energies as compared to the case with no sterile states present.
The number of states that can be accessed depends on the mass of the sterile states. The neutrinos produced in the β-decays can only oscillate into sterile states with a lower mass than the energy available from the decay, thus only states si with $m_{si} < E_0$ are

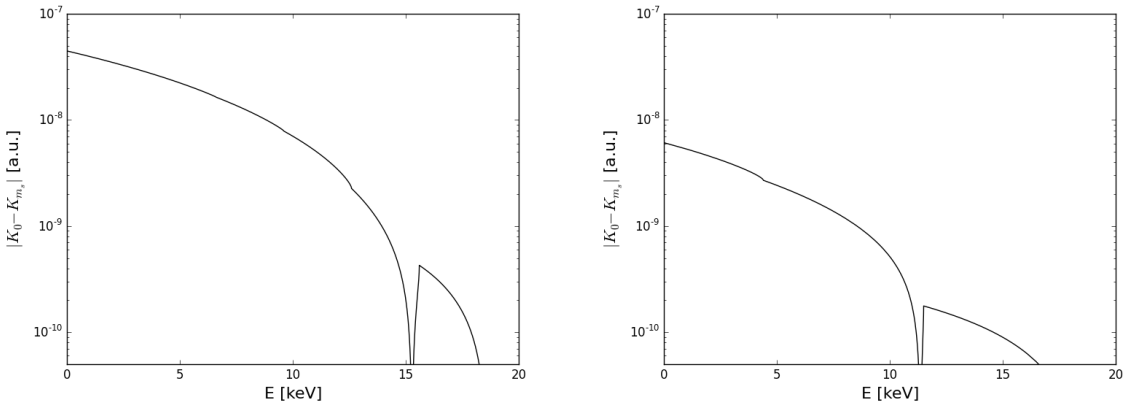

Figure 6.3: The differences between the Kurie functions without (K_0) and with (K_{m_s}) a sterile neutrino tower are shown for two exmples on a logarithmic scale. **Left:** Influence of a tower with $m_{s1} = 3$ keV and $\sin^2 2\theta_1 = 4 \cdot 10^{-10}$ on the Kurie function. The neutrino energy allows them to access the lightest four states. **Right:** This tower has $m_{s1} = 7.1$ keV and $\sin^2 2\theta_1 = 7 \cdot 10^{-11}$. Only the two lightest states are accessible.

accessible.

A different question is how many states can actually be measured. This depends on how much the presence of the sterile state changes the β spectrum, i.e. how pronounced the kink is. This then depends on the mixing angle.

An upgraded version of KATRIN for sterile neutrinos for three years could probe mixing angles down to $\sin^2 2\theta \approx 4 \cdot 10^{-8}$ for a mass range of $5\,\text{keV} < m_s < 15$ keV and $\sin^2 2\theta \approx 1 \cdot 10^{-7}$ for a wider mass range of $3\,\text{keV} < m_s < 17\,\text{keV}$. With this performance, none of the sterile neutrino states investigated here would be observable in the near future.

6.3 Observability of sterile neutrinos with β-decay experiments

The β-decay of tritium is well-suited to determine the absolute mass scale of the neutrino. With the same general setup as for the light neutrino mass search near the endpoint E_0 of the spectrum, and a different detector setup, tritum decay can also be used to probe the sterile neutrino parameters. KATRIN, designed to determine m_β at the sub-eV scale, is a prime candidate for an upgrade to search for sterile neutrinos. However, the expected sensitivity of such a detector would not allow to probe much of the cosmologically intersting region where mixing angles $\sin^2 2\theta < 10^{-8}$. Likewise, it

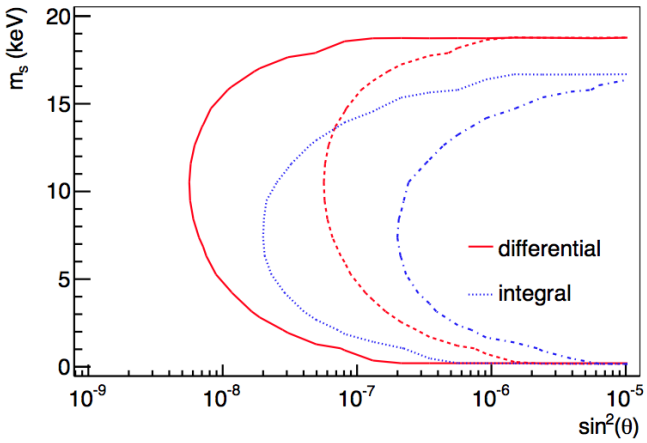

Figure 6.4: Proposed 90 % exclusion limits after three years of data taking with an upgraded KATRIN experiment for a differential measurement at full source strength (red solid), a differential measurement at 1 % of the full source strength (red dashed), an integrated measurement at full source strength (blue dotted) and an integrated mesurement at 1 % of the full source strength (blue dash-dotted). Taken from [63].

would not be sensitive to the examples of sterile neutrino states presented in this thesis, see Figure 6.4. But, as the present bounds only reach $\sin^2 2\theta \sim 10^{-3}$ [25], the upgrade under discussion would probe a large region of the parameter space not yet kinematically probed. The authors of [63] study the sensitivity of an upgraded KATRIN experiment running for three years for two ways of measurement. In the integral measurement, the filter potential is varied for each measurement point, such that only electrons with an energy higher than the filter potential hit the detector, and all electrons with energies higher than the filter potential are measured. In the differential spectrum, the retarding potential is set to low values, such that almost the full spectrum reaches the detector. The detector itself needs to provide an energy resolution which allows to identify the narrow regions of kinks.

The lightest sterile state has the largest impact on the β spectrum (i.e. most pronounced kink), therefore the first sterile state will be most easily accessible by experiments. If sterile neutrinos are found, it would make sense to extend the search to higher KK modes. Searches with β-decay experiments are model independent in the sense that they do not depend on cosmological models. Also, there are no processes known to produce kink-like features in the spectrum and imitate a sterile neutrino. On the other hand, β-decay experiments are only sensitive to sterile neutrinos that mix with electron neutrinos.

An additional aspect worth mentioning is the meaning of finding sterile neutrinos with

an upgraded KATRIN in a parameter space that is excluded by X-ray bounds. In that case a possible conclusion is that there is more than just sterile neutrinos out there. If the possibility of RH currents to exist right outside the regions excluded by the LHC, i.e. $m_{W_R} \gtrsim 2.5$ GeV is taken into account, and the lepton mixing is large in the RH sector between electrons and the sterile neutrino DM candidate, the mixing may be well within reach of the upgrated KATRIN. At the same time, the RH current provides a new decay mode for the sterile neutrinos involving the mixing of LH states to RH currents. The mixing, however, could be small enough to avoid conflict with the X-ray bounds. As a result, the contribution of sterile neutrinos to the β-decay contribution would get enhanced while the contribution to DM decay is negligible. This was recently shown in [64].

Chapter 7

Conclusion and outlook

Sterile neutrinos arise in many extensions of the SM and each extension has its own variation of sterile neutrinos. Some are very light (eV mass scale) and can solve reactor anomalies, some are very heavy (10^{15} GeV) and explain via the seesaw mechanism why active neutrinos are so light, and yet others are in the intermediate mass scale and are good candidates for Warm Dark Matter. In this thesis we focused on the latter and studied what effect an extra dimensional setting has on the sterile neutrino abundance and on possible sterile neutrino signatures. We introduced just one additional sterile neutrino, and allowed it to only mix with one active neutrino flavor. We then introduced one effective compactified extra dimension and saw how the one sterile neutrino splits into an infinite tower of modes with ever increasing mass. The beauty of this model is that the mass of each state and its mixing with the active sector is fully determined by the radius of the extra dimension. The mass of the k-th mode is given by $m_{sk} \sim k/R$, where R is the compactification radius of the ED, and its mixing to the active state is $\propto k^{-2}$.

We presented two production mechanisms of sterile neutrinos, the Dodelson-Widrow and the Shi-Fuller mechanism. The former is based on the mixing between active and sterile states, resulting in an abundance of sterile neutrinos building up in thermal equilibrium. The latter makes use of the resonant enhancement of oscillations in dense, asymmetric matter, which leads to a conversion of flavors and can largely increase the sterile neutrino abundance. As we were mainly interested in the effect of the tower, we allowed for the sterile neutrino to mix with only one active flavor to make the description easier. We saw that the higher KK modes have no significant contribution to the total sterile neutrino abundance, if we require that abundance to match the observed DM density and restrict ourselves to the parameter space that is not excluded by X-ray observations. We next

examined the lifetimes and decay modes of the sterile neutrino tower. The visible decay mode $\nu_s \to \nu_\alpha \gamma$ is the channel with the highest discovery potential, and is currently being searched for in form of weak and previously unidentified mono-energetic spectral lines coming from objects with a high DM density like galaxy clusters, dwarf galaxies etc.

It is from the astrophysical search that a observation of a 7.1 keV sterile neutrino decay line was proposed earlier this year. The status of this 3.55 keV line found in stacked spectra of galaxy clusters and independently in galactic spectra is not conclusive and more observations are needed to settle the question of the nature of the line. Its interpretation is difficult, and may be strongly affected by the modelling of the background. It may turn out that the line is of astrophysical origin. While it is thus easiest to detect a new feature with astronomic observations, it is difficult to establish the findings as originating from new physics without the confirmation from other forms of measurements. Therefore, other searches, even if less promising, should be explored. One of those possibilities is a search for derivations from the emission spectrum of β-decay electrons expected from a three neutrino flavor scenario. Here, the earliest results can be expected sometime after 2020. By that time, the nature of the 3.55 keV line should be settled (at least it should be known whether it can or cannot be explained astrophysically), and other new findings might be incompatible with astrophysical origins.

We have shown that a possible β-decay search for sterile neutrinos will probably not reach the sensitivity of finding the sterile neutrino examples discussed in this thesis. It could still probe some of the astrophysically favored parameter space.

The main conclusion from this work is, that an extra dimensional setting does not significantly change the phenomenology of sterile neutrino dark matter. In the model considered here it turns out that the vast majority of the sterile neutrino abundance is accounted for by the lightest state. Moreover, as the higher modes only have a negligible contribution to the sterile neutrino abundance, their discovery in the next few years is highly unlikely. Likewise, a discovery of multiple states with a β-decay experiment is unlikely, unless we assume additional new physics like right-handed currents. This last conclusion, however, only holds true for a WDM candidate sterile neutrino. If the sterile neutrino is not the main DM constituent, the astrophysical bounds do not apply. In that case, it is possible that e.g. the mixing between the electron-flavor and sterile states is larger than assumed here. Then, not only the prospects of finding one sterile neutrino with a β-decay experiment would be better, but also the prospects of finding the second mode – or excluding its existence. Another possibility is of course, that the sterile neutrinos do account for the DM, but the generation mechanism of their present-day

abundance is more complicated than the simple mechanism presented here. Then the relative contribution of the higher modes to the overall abundance may be enhanced, e.g. by allowing for an initial overproduction of the lightest state with subsequent dilution by entroy injection from the decay of some heavy, unstable particle.
In this thesis, the sterile neutrinos were assumed to mix with only one active state. The picture for sterile neutrino production in the Early Universe should not change if the sterile neutrinos mix with all active states. The mixing depends on the mass squared difference between the active and sterile state, and thus is approximately the same for all three flavors. We can sum up all admixtures of the active states to the sterile mass state and combine all mixings into an effective acitve-sterile mixing angle, arriving at the exact same description of the process as for only one mixing angle. The lepton asymmetries can again be summarized into one effective lepton asymmetry, leaving our description and results unchanged. For the signatures from β dacays, however, a different mixing pattern might have a large effect. It is the electron-sterile mixing that determines the effect of the sterile neutrino on the β-spectrum. If this mixing angle is much smaller than the effective active-sterile mixing angle, so is the prospect of finding the sterile neutrino with β-decay.
To conclude, while the prospects to find a sterile neutrino (and identify it as such) in the years to come are good, the question of whether a sterile neutrino has higher KK modes will likely not be answered anytime soon.

Acknowledgements

First of all I want to thank my supervisor Werner Rodejohann for giving me the opportunity to write this thesis, for pushing me back in the right direction when I was lost in my way. I am also thankful that he sent me to the Heraeus-Seminar on massive neutrinos and the SAT astroparticle school.
I also want to thank Manfred Lindner and all group members for creating the nice atmosphere and welcoming me to share it. Especially, I want to thank He Zhang for his patience with me and for helping me to get settled in the extra-dimensional framework and Julian Heeck for fruitful discussions.
Thank you, my office mates for discussions, jokes, and sharing a grad student's hopes, dreams and sorrows — in order of (dis)appearance Johannes Welter, Steffen Schmidt, Ludwig Rauch, Tim Wolf, Meike Danisch, Natascha Rupp, Thomas Rink, Miguel Campos, Alexander Helmboldt and Dominick Cichon.
I am especially grateful to Martin Holthausen, Alexander Helmboldt, Johannes Welter and Miguel Campos for proofreading this thesis.
Thank you my dear friends Bea, Franzi and Sebastian for the fun times we shared, for staying in touch when we were far apart — I hope we will once more. Bea, thank you for your help and for always cheering me up.
A very special thank you goes to my parents, who have always supported me in every decision I made, dziękuję, kochani. Tyler, thank you for always being there for me.

Bibliography

[1] Angloher, G., et al. *Results on low mass WIMPs using an upgraded CRESST-II detector* (2014). 1407.3146 ; Beltrame, P. *Direct Dark Matter search with the XENON program*. 143–148 (2013). 1305.2719 .

[2] Kraus, C., Bornschein, B., Bornschein, L., et al. *Final results from phase II of the Mainz neutrino mass search in tritium beta decay*. Eur.Phys.J., C40, 447–468 (2005). hep-ex/0412056 ; Aseev, V., et al. *An upper limit on electron antineutrino mass from Troitsk experiment*. Phys.Rev., D84, 112003 (2011). 1108.5034 .

[3] de Gouvea, A., et al. *Working Group Report: Neutrinos* (2013). 1310.4340 .

[4] Boyarsky, A., Ruchayskiy, O., Iakubovskyi, D., et al. *An unidentified line in X-ray spectra of the Andromeda galaxy and Perseus galaxy cluster* (2014). 1402.4119 .

[5] Bulbul, E., Markevitch, M., Foster, A., et al. *Detection of an Unidentified Emission Line in the Stacked X-Ray Spectrum of Galaxy Clusters*. ApJ, 789, 13 (2014). 1402.2301 .

[6] Arkani-Hamed, N., Dimopoulos, S., Dvali, G. *The Hierarchy problem and new dimensions at a millimeter*. Phys.Lett., B429, 263–272 (1998). hep-ph/9803315 .

[7] Aguilar-Arevalo, A., et al. *Evidence for neutrino oscillations from the observation of anti-neutrino(electron) appearance in a anti-neutrino(muon) beam*. Phys.Rev., D64, 112007 (2001). hep-ex/0104049 .

[8] Aguilar-Arevalo, A., et al. *Event Excess in the MiniBooNE Search for $\bar{\nu}_\mu \to \bar{\nu}_e$ Oscillations*. Phys.Rev.Lett., 105, 181801 (2010). 1007.1150 .

[9] Mention, G., Fechner, M., Lasserre, T., et al. *The Reactor Antineutrino Anomaly*. Phys.Rev., D83, 073006 (2011). 1101.2755 .

[10] Abdurashitov, J., et al. *Measurement of the solar neutrino capture rate with gallium metal. III: Results for the 2002–2007 data-taking period*. Phys.Rev., C80, 015807 (2009). 0901.2200 ; Kaether, F., Hampel, W., Heusser, G., et al. *Reanalysis of the GALLEX solar neutrino flux and source experiments*. Phys.Lett., B685, 47–54 (2010). 1001.2731 .

[11] Kopp, J., Maltoni, M., Schwetz, T. *Are there sterile neutrinos at the eV scale?*. Phys.Rev.Lett., 107, 091801 (2011). 1103.4570 .

[12] Ade, P., et al. *Planck 2013 results. XVI. Cosmological parameters*. Astron.Astrophys. (2014). 1303.5076 .

[13] de Gouvea, A., et al. *Working Group Report: Neutrinos* (2013). 1310.4340 .

[14] Peskin, M. E., Schroeder, D. V. *An Introduction To Quantum Field Theory*, (Westview Press 1995).

[15] Zuber, K. *Neutrino Physics*. Series in High Energy Physics, Cosmology and Gravitation, (IoP 2004).

[16] Mohapatra, R., Pal, P. *Massive Neutrinos in Physics and Astrophysics*. Lecture Notes in Physics Series, (World Scientific 2004).

[17] Povh, B., Rith, K., Scholz, C., et al. *Teilchen und Kerne: Eine Einfhrung in die physikalischen Konzepte; 9th ed*, (Springer Spektrum 2013).

[18] Smirnov, A. Y. *The MSW effect and solar neutrinos*. hep-ph/0305106 .

[19] Maki, Z., Nakagawa, M., Sakata, S. *Remarks on the unified model of elementary particles*. Prog.Theor.Phys., 28, 870–880 (1962).

[20] Nordström, G. *Über die Möglichkeit, das elektromagnetische Feld und das Gravitationsfeld zu vereinigen*. Physik. Zeitschrift, 15 (1914).

[21] Kaluza, T. *On the Problem of Unity in Physics*. Sitzungsber. Preuss. Akad. Wiss. Berlin (Math.Phys.), 1921, 966–972 (1921); Klein, O. *Quantum theory and five-dimensional relativity theory*. Z. Phys., 37 (1926); Klein, O. *The atomicity of electricity as a quantum theory law*. In *The Oskar Klein Memorial Lectures*, (World Scientific1991). Article originally published in Nature, 118 (1926).

[22] Dienes, K. R., Dudas, E., Gherghetta, T. *Extra space-time dimensions and unification*. Phys.Lett., B436, 55–65 (1998). hep-ph/9803466 .

[23] Dienes, K. R., Dudas, E., Gherghetta, T. *Neutrino oscillations without neutrino masses or heavy mass scales: A Higher dimensional seesaw mechanism*. Nucl.Phys., B557, 25 (1999). hep-ph/9811428 .

[24] Kapner, D. J., Cook, T. S., Adelberger, E. G., et al. *Tests of the gravitational inverse-square law below the dark-energy length scale*. Phys. Rev. Lett., 98, 021101 (2007).

[25] Olive, K., et. al., (PDG). Chin. Phys. C, 38, 090001 (2014). URL `http://pdg.lbl.gov`.

[26] Rodejohann, W., Zhang, H. *Signatures of extra dimensional sterile neutrinos*. Phys. Lett., B737, 81 – 89 (2014).

[27] Barry, J., Rodejohann, W., Zhang, H. *Sterile Neutrinos for Warm Dark Matter and the Reactor Anomaly in Flavor Symmetry Models*. JCAP, 1201, 052 (2012). 1110.6382 .

[28] Merle, A., Niro, V. *Deriving Models for keV sterile Neutrino Dark Matter with the Froggatt-Nielsen mechanism*. JCAP, 1107, 023 (2011). 1105.5136 .

[29] Kusenko, A., Takahashi, F., Yanagida, T. T. *Dark Matter from Split Seesaw*. Phys.Lett., B693, 144–148 (2010). 1006.1731 .

[30] Zhang, H. *Light Sterile Neutrino in the Minimal Extended Seesaw*. Phys.Lett., B714, 262–266 (2012). 1110.6838 .

[31] Merle, A. *keV Neutrino Model Building*. Int.J.Mod.Phys., D22, 1330020 (2013). 1302.2625 .

[32] Shi, X., Fuller, G. M. *New dark matter candidate: Nonthermal sterile neutrinos*. Phys. Rev. Lett., 82, 2832–2835 (1999). 9810076 .

[33] Abazajian, K., Fuller, G. M., Patel, M. *Sterile neutrino hot, warm, and cold dark matter*. Phys.Rev., D64, 023501 (2001). astro-ph/0101524 .

[34] Kusenko, A. *Sterile neutrinos: the dark side of the light fermions*. Phys. Rept., 481, 1–28 (2009). 0906.2968 .

[35] Bezrukov, F., Hettmansperger, H., Lindner, M. *keV sterile neutrino Dark Matter in gauge extensions of the Standard Model*. Phys. Rev., D81, 085032 (2010). 0912.4415 .

[36] Abazajian, K., Fuller, G. M., Tucker, W. H. *Direct detection of warm dark matter in the X-ray*. Astrophys.J., 562, 593–604 (2001). astro-ph/0106002 .

[37] Viel, M., Becker, G. D., Bolton, J. S., et al. *Warm dark matter as a solution to the small scale crisis: New constraints from high redshift Lyman-? forest data*. Phys.Rev., D88, 043502 (2013). 1306.2314 .

[38] Dodelson, S., Widrow, L. M. *Sterile-neutrinos as dark matter*. Phys.Rev.Lett., 72, 17–20 (1994). hep-ph/9303287 .

[39] Kolb, E. W., Turner, M. S. *The Early Universe*. Frontiers in Physics, (Westview Press 1994).

[40] Nötzold, D., Raffelt, G. *Neutrino Dispersion at Finite Temperature and Density*. Nucl.Phys., B307, 924 (1988).

[41] Wolfenstein, L. *Neutrino Oscillations in Matter*. Phys.Rev., D17, 2369–2374 (1978); Wolfenstein, L. *Neutrino Oscillations and Stellar Collapse*. Phys.Rev., D20, 2634–2635 (1979); Mikheev, S., Smirnov, A. Y. *Resonance Amplification of Oscillations in Matter and Spectroscopy of Solar Neutrinos*. Sov.J.Nucl.Phys., 42, 913–917 (1985); Mikheev, S., Smirnov, A. Y. *Resonant amplification of neutrino oscillations in matter and solar neutrino spectroscopy*. Nuovo Cim., C9, 17–26 (1986); Smirnov, A. Y. *The MSW effect and solar neutrinos*. 23–43 (2003). hep-ph/0305106 .

[42] Simha, V., Steigman, G. *Constraining The Universal Lepton Asymmetry*. JCAP, 0808, 011 (2008). 0806.0179 .

[43] Kishimoto, C. T., Fuller, G. M., Smith, C. J. *Coherent Active-Sterile Neutrino Flavor Transformation in the Early Universe*. Phys.Rev.Lett., 97, 141301 (2006). astro-ph/0607403 .

[44] Dolgov, A. D. *Neutrinos in cosmology*. Phys. Rep., 370, 333–535 (2002). hep-ph/0202122 .

[45] Garrison-Kimmel, S., Rocha, M., Boylan-Kolchin, M., et al. *Can Feedback Solve the Too Big to Fail Problem?* (2013). 1301.3137 .

[46] Bond, J. R., Efstathiou, G., Silk, J. *Massive neutrinos and the large-scale structure of the universe*. Phys. Rev. Lett., 45, 1980–1984 (1980). URL http://link.aps.org/doi/10.1103/PhysRevLett.45.1980.

[47] Pal, P. B., Wolfenstein, L. *Radiative decays of massive neutrinos*. Phys. Rev. D, 25, 766–773 (1982).

[48] Boyarsky, A., Franse, J., Iakubovskyi, D., et al. *Checking the dark matter origin of 3.53 keV line with the Milky Way center* (2014). 1408.2503 .

[49] Malyshev, D., Neronov, A., Eckert, D. *Constraints on 3.55 keV line emission from stacked observations of dwarf spheroidal galaxies*. Phys.Rev., D90, 10, 103506 (2014). 1408.3531 .

[50] Anderson, M. E., Churazov, E., Bregman, J. N. *Non-Detection of X-Ray Emission From Sterile Neutrinos in Stacked Galaxy Spectra* (2014). 1408.4115 .

[51] Riemer-Sorensen, S. *Questioning a 3.5 keV dark matter emission line* (2014). 1405.7943 .

[52] Jeltema, T. E., Profumo, S. *Dark matter searches going bananas: the contribution of Potassium (and Chlorine) to the 3.5 keV line* (2014). 1408.1699 .

[53] Iakubovskyi, D. *New emission line at 3.5 keV - observational status, connection with radiatively decaying dark matter and directions for future studies* (2014). 1410.2852 .

[54] Lovell, M. R., Bertone, G., Boyarsky, A., et al. *Decaying dark matter: the case for a deep X-ray observation of Draco* (2014). 1411.0311 .

[55] Carlson, E., Jeltema, T., Profumo, S. *Where do the 3.5 keV photons come from? A morphological study of the Galactic Center and of Perseus* (2014). 1411.1758 .

[56] Ishida, H., Jeong, K. S., Takahashi, F. *7 keV sterile neutrino dark matter from split flavor mechanism*. Phys.Lett., B732, 196–200 (2014). 1402.5837 ; Abazajian, K. N. *Resonantly-Produced 7 keV Sterile Neutrino Dark Matter Models and the Properties of Milky Way Satellites*. Phys.Rev.Lett., 112, 161303 (2014). 1403.0954 ; Merle, A., Schneider, A. *Production of Sterile Neutrino Dark Matter and the 3.5 keV line* (2014). 1409.6311 ; Patra, S., Pritimita, P. *7 keV sterile neutrino Dark Matter in extended seesaw framework* (2014). 1409.3656 .

[57] Higaki, T., Jeong, K. S., Takahashi, F. *The 7 keV axion dark matter and the X-ray line signal*. Phys.Lett., B733, 25–31 (2014). 1402.6965 ; Jaeckel, J., Redondo, J., Ringwald, A. *3.55 keV hint for decaying axionlike particle dark matter*. Phys.Rev., D89, 10, 103511 (2014). 1402.7335 ; Lee, H. M., Park, S. C., Park, W.-I. *Cluster X-ray line at* 3.5 keV *from axion-like dark matter*. Eur.Phys.J., C74, 9, 3062 (2014). 1403.0865 ; Cicoli, M., Conlon, J. P., Marsh, M. C. D., et al. *A 3.55 keV Photon Line and its Morphology from a 3.55 keV ALP Line*. Phys.Rev., D90, 023540 (2014). 1403.2370 .

[58] Babu, K., Mohapatra, R. N. *7 keV Scalar Dark Matter and the Anomalous Galactic X-ray Spectrum*. Phys.Rev., D89, 115011 (2014). 1404.2220 .

[59] Park, J.-C., Park, S. C., Kong, K. *X-ray line signal from 7 keV axino dark matter decay*. Phys.Lett., B733, 217–220 (2014). 1403.1536 ; Choi, K.-Y., Seto, O. *X-ray line signal from decaying axino warm dark matter*. Phys.Lett., B735, 92 (2014). 1403.1782 ; Kolda, C., Unwin, J. *X-ray lines from R-parity violating decays of keV sparticles*. Phys.Rev., D90, 023535 (2014). 1403.5580 .

[60] Cline, J. M., Farzan, Y., Liu, Z., et al. *3.5 keV X-rays as the "21 cm line" of dark atoms, and a link to light sterile neutrinos*. Phys.Rev., D89, 121302 (2014). 1404.3729 .

[61] Osipowicz, A., et al. *KATRIN: A Next generation tritium beta decay experiment with sub-eV sensitivity for the electron neutrino mass. Letter of intent* (2001). hep-ex/0109033 .

[62] Otten, E. *The long route to katrin – neutrino mass in β-decay* (2014). URL `http://qgp.uni-muenster.de/~weinheim/heraeus_seminar561/talks/02_Tuesday/04_Otten_The_long_Route_to_KATRIN_Bad_Honnef_2014.pdf`. Talk given at 561.WE-Heraeus Seminar (2014).

[63] Mertens, S., Lasserre, T., Groh, S., et al. *Sensitivity of Next-Generation Tritium Beta-Decay Experiments for keV-Scale Sterile Neutrinos* (2014). 1409.0920 .

[64] Barry, J., Heeck, J., Rodejohann, W. *Sterile neutrinos and right-handed currents in KATRIN*. JHEP, 1407, 081 (2014). 1404.5955 .

Erklärung:

Ich versichere, dass ich diese Arbeit selbstständig verfasst habe und keine anderen als die angegebenen Quellen und Hilfsmittel benutzt habe.

Heidelberg, den (Datum) .....